

Market Segmentation Trees

Ali Aouad

London Business School, London, UK, aaouad@london.edu

Adam N. Elmachtoub

Department of Industrial Engineering and Operations Research and Data Science Institute, Columbia University, New York, NY, adam@ieor.columbia.edu

Kris J. Ferreira

Harvard Business School, Harvard University, Boston, MA, kferreira@hbs.edu

Ryan McNellis

Department of Industrial Engineering and Operations Research and Data Science Institute, Columbia University, New York, NY, rtm2130@columbia.edu

We seek to provide an interpretable framework for segmenting users in a population for personalized decision-making. The standard approach is to perform market segmentation by clustering users according to similarities in their contextual features, after which a “response model” is fit to each segment in order to model how users respond to personalized decisions. However, this methodology is not ideal for personalization, since two users could in theory have similar features although their response behaviors are different. We propose a general methodology, *Market Segmentation Trees* (MSTs), for learning interpretable market segmentations explicitly driven by identifying differences in user response patterns. To demonstrate the versatility of our methodology, we design two new, specialized MST algorithms: (i) Choice Model Trees (CMTs) which can be used to predict a user’s choice amongst multiple options, and (ii) Isotonic Regression Trees (IRTs) which can be used to solve the bid landscape forecasting problem. We provide a customizable, open-source code base for training MSTs in Python which employs several strategies for scalability, including parallel processing and warm starts. We provide a theoretical analysis of the asymptotic running times of our algorithmic methods, which validates their computational tractability on large datasets. We assess the practical performance of MSTs on several synthetic and real world datasets, showing that our method reliably finds market segmentations which accurately model response behavior. Further, when applying MSTs to historical bidding data from a leading demand-side platform (DSP), we show that MSTs consistently achieve a 5-29% improvement in bid landscape forecasting accuracy over the DSP’s current model, on various commonly-used accuracy metrics. Our findings indicate that integrating market segmentation with response modeling consistently leads to improvements in response prediction accuracy, thereby aiding personalization. Further, we demonstrate that this integrated, interpretable approach is computationally tractable on large-scale datasets. Our open-source implementation is readily usable by practitioners.

Key words: market segmentation, business analytics, decision trees

1. Introduction

Recent growth of online commerce and media consumption have resulted in an expansion of opportunities for firms to engage in personalized decision-making. Online retailers such as Amazon offer product recommendations on their homepage, which are personalized using the visiting user’s purchase history and demographic information. Streaming services such as Hulu, YouTube, and Spotify personalize ads based on the media content being consumed and other aspects of the user’s activity history. Online search engines such as Google personalize the ranking of search results based on user’s activity history. In online advertising exchanges, bids for online ad spots can be customized on the basis of various features encoding the ad spot and the site visitor.

Personalized decision-making often lies at the intersection of two fundamental technical challenges: *market segmentation* (clustering users into segments based on user characteristics) and *response modeling* (the probabilistic modeling of a user’s response to a personalized decision). For example, if an online platform wishes to personalize the ads displayed to its users in order to maximize the click-through rate, it could (1) segment users into interpretable and homogeneous segments, and (2) model the click behavior of users in each segment. One common approach is to perform the tasks of market segmentation and response modeling separately, using a clustering algorithm (e.g., *K*-means) for market segmentation and then fitting a response model (e.g., logistic regression) within each cluster (Yang et al. 2016). However, such a market segmentation is driven only by user feature dissimilarity rather than differences in user response behavior.

We propose a general methodology, Market Segmentation Trees (MSTs), that builds interpretable decision trees for *joint* market segmentation and response modeling, which can be used for a variety of personalized decision-making applications. Decision tree splits are applied by the MST to segment the market according to available *contextual* attributes for personalization (e.g., features encoding the user). A response model is fit in each segment to probabilistically model the users’ response (e.g., clicks) as a function of the decision variables (e.g., ads that were displayed). We propose a training procedure for MSTs in which decision tree splits are decided through optimizing the predictive accuracy of the resulting collection of response models. Thus, our training procedure yields a market segmentation driven by accurately capturing differences in user response behavior.

We emphasize that a primary motivation for the use of decision trees for tackling this problem is due to their interpretability (in addition to their strong predictive performance). Increasingly, companies are being held more accountable for their data-driven decisions by both consumers and regulators (Goodman and Flaxman 2017). Decision trees provide a simple way to visualize the decision-making stream, and have been used in a variety of settings (Kallus 2017, Elmachtoub et al. 2017, Ciocan and Mišić 2018, Bertsimas et al. 2019). In our setting, the decision for every user

corresponds to a single response model, which is selected by simply observing where the user’s context falls in the tree.

We provide an open-source implementation of our training procedure in Python (Aouad et al. [n. d.]). The code base is modular and easily customizable to fit different personalized decision-making applications. Several features have been included for improved scalability, including the option of using parallel processing and warm starts for training the MST models. We provide a theoretical analysis of the code’s asymptotic computational complexity supporting its tractability in large data settings. Specifically, we show that under mild conditions, the implementation’s computational complexity is *linear* in the depth of the learned MST; moreover, the impact of tree depth on computational complexity can be greatly diminished or even nullified if a sufficient number of cores are available for parallel processing.

To demonstrate the versatility of our methodology, we design two new, specialized MST algorithms. First, we propose a new algorithm, *Choice Model Trees* (CMTs), which can be used to predict a user’s choice amongst multiple options. Our model uses decision tree splits to segment users on the basis of their features (e.g., prior purchase history), and within each segment a Multinomial Logit (MNL) choice model is fit as the response model to predict the probability that users in that segment choose each option. We examine the performance of CMTs on a variety of synthetic datasets, observing that CMTs reliably find market segmentations which accurately predict choice probabilities, whereas other natural benchmarks do not. Furthermore, we show that CMTs are more easily able to overcome model misspecification and are quite robust to overfitting. Next, we apply the CMT to a dataset of hotel searches on Expedia made publicly available (ICDM 2013). The CMT uses available features about the user and search query for the purposes of market segmentation, including the number of adults and children in the party and the queried length of stay. We find that the CMT consistently outperforms other natural benchmarks by 0.53-2.2% with respect to hotel booking predictive accuracy, while also providing an interpretable segmentation.

We also propose a second algorithm derived from our MST framework, *Isotonic Regression Trees* (IRTs), which can be used to solve the bid landscape forecasting problem. A “bid landscape” refers to the probability distribution of the highest (outside) bid that an ad spot will receive when being auctioned at an advertising exchange. The bid landscape forecasting problem is important to Demand Side Platforms (DSPs) – ad campaign management platforms – in estimating the minimum bid necessary to win different types of ad spots. A significant challenge is presented when ad spot transactions occur through first-price auctions – in such cases the highest outside bid is never revealed, and the DSP only sees whether their submitted bid resulted in an auction win or loss outcome. We propose a new model, IRTs, for the bid landscape forecasting problem under first-price auction dynamics. Our model uses a decision tree to segment auctions according to features about

the visiting user (e.g., user’s location) and the ad spot being auctioned (e.g., width/height in pixels). An isotonic regression model is used as the response model to forecast the bid landscapes of the auctions within each segment. IRTs are fully non-parametric, operating without assumptions about the distribution of the bid landscapes or of their relationship with the auction features. We apply our IRT to an ad spot transaction dataset collected by a large DSP provider, and we demonstrate that our model consistently achieves a 5-29% improvement in bid landscape forecasting accuracy over the DSP’s current approach across multiple ad exchanges (for confidentiality reasons, the name of the DSP provider is not reported in this paper).

2. Literature Review

In this work, we propose a general framework (MSTs) for building decision trees for the purposes of market segmentation and personalized decision-making. An introduction to decision trees may be found in Friedman et al. (2001). MSTs take the structural form of model trees, which refer to a generalization of decision trees that allow for non-constant leaf prediction models. Arguably the most common model tree algorithms explored in the literature are linear model trees (Quinlan et al. 1992) and logistic model trees (Chan and Loh 2004, Landwehr et al. 2005), which propose using linear and logistic regression leaf models with decision trees. Zeileis et al. (2008) develop a general framework, model-based recursive partitioning (MOB), for training model trees with parametric leaf models such as linear and logistic regression. Unlike our training methodology, none of the above methods select decision tree splits which *directly* minimize the predictive error of the resulting collection of leaf models, instead employing heuristic splitting criterion such as class purity (Chan and Loh 2004, Landwehr et al. 2005) and parameter instability (Zeileis et al. 2008). We believe this is due to a presumed computational intractability associated with identifying the split that directly minimizes prediction error, as the predictive evaluation of each split would entail fitting multiple leaf models to the training data. We demonstrate that through efficient use of parallel processing, model trees may be tractably trained through our direct split optimization procedure, and we provide a novel computational complexity analysis supporting its tractability in Section 3.3.4.

We are among the first to propose using model trees for market segmentation and for personalized decision-making problems. Similar to our CMT algorithm, Mišić (2016) proposes using model trees with choice model leaves for personalizing assortment decisions. In contrast, MSTs offer a more general framework for building model trees for market segmentation in areas outside of assortment optimization. Moreover, we develop an open-source implementation, which has been empirically validated on large-scale real-world datasets. Kallus (2017) and Bertsimas et al. (2019) propose methodology for training decision trees for segmenting customers and personalizing treatments across the resulting segments. Each treatment option is associated with an unknown and customer-variant

expected reward, and the authors provide recursive partitioning and integer programming strategies for training the trees to maximize the rewards from the prescribed treatments. The treatment options are assumed to belong to a small set of feasible values and thus response models are not needed – the expected reward associated with each treatment option may be independently estimated by averaging the rewards observed when the treatment was applied historically. MSTs generalize the decision tree methods proposed by Kallus (2017) and Bertsimas et al. (2019) by supporting continuous and high-dimensional decision spaces by way of response models.

The market segmentation produced by MSTs attempts to maximize the predictive accuracy of the resulting collection of response models (i.e., leaf models). Conversely, the typical approach in industry is to perform the tasks of market segmentation and response modeling separately, first clustering users according to closeness in their contextual attributes and then fitting response models within each cluster (Yang et al. 2016). A popular method for doing so is K -means clustering – an unsupervised machine learning algorithm which attempts to find the clustering of users that minimizes the variance of the contextual features within in each cluster. K -means clustering is widely utilized for the purposes of market segmentation – Tuma et al. (2011) found that K -means clustering was the most frequently-used market segmentation approach across 210 research articles applying clustering methods for market research (44.25% of all articles). The method is taught in many popular textbooks on marketing research often used today (Malhotra et al. 2006, Churchill and Iacobucci 2006). Ettl et al. (2019) employ this procedure in segmenting airline customers on the basis of their personal information and booking data, afterwards fitting logistic regression models in each cluster for the purposes of personalizing bundles of product offers. We argue that the K -means clustering approach suffers from a fundamental limitation – namely, the resulting market segmentation does not take into account the predictive accuracy of the resulting collection of response models but is instead driven only by minimizing within-cluster feature dissimilarity. We show through numerical experiments in Section 4 that integrating market segmentation with response modeling can lead to significant improvements in the predictive accuracy of user responses, thereby aiding personalization.

There have been several non-tree-based approaches proposed in the literature for jointly performing market segmentation and response modeling. One of the most popular approaches is the latent-class multinomial logit model (LC-MNL) originally proposed by Kamakura and Russell (1989). The LC-MNL model assumes the existence of K different market segments (with the value of K chosen by the practitioner), with each segment having a separate MNL for modeling response behavior. In Kamakura and Russell (1989), all customers are modeled as having the same segment-membership probabilities; Gupta and Chintagunta (1994) and Kamakura et al. (1994) extend the LC-MNL

model to allow the segment-membership probabilities to be a function of customer-specific features, specifically in the following manner:

$$\mathbb{P}(\text{Segment} = k | x) = \frac{e^{\gamma_k^T x}}{\sum_{k'=1}^K e^{\gamma_{k'}^T x}}$$

Above, x denotes the contextual attributes for the customer, $k \in \{1, \dots, K\}$ denotes a particular market segment, and $\gamma_1, \dots, \gamma_K$ are parameter vectors to be estimated from data. Note that each customer attribute is assumed to have a monotonic relationship with respect to the segment-membership probabilities, and that more generally the relationship between contexts and segment-membership probabilities are constrained to take a specific functional (parametric) form. Conversely, MSTs perform market segmentation using nonparametric decision tree splits which can flexibly capture non-monotonic and complex mappings from contexts to segments. Also, MSTs naturally learn interactions between contexts in mapping users to segments, whereas contextual interaction terms would have to be manually specified in the LC-MNL model. Furthermore, MSTs provide a more interpretable market segmentation in that each user is in exactly one segment, rather than probabilistically in each segment in the LC-MNL model. Finally, LC-MNL models are typically fit using Expectation-Maximization (EM) methods which are known to be prohibitively slow on large datasets (Jagabathula et al. 2018a). We found in our own numerical experiments that the LC-MNL model (as implemented by the R package `gmnl`) did not run successfully on our datasets as the computational time and memory resources required were too prohibitive for the hardware available.

Bernstein et al. (2018) propose a *dynamic* market segmentation approach which adaptively adjusts customer segments and their associated response models as more observations are collected. The authors use a Bayesian semi-parametric framework called the *Dirichlet Process Mixture* to model the customers' preferences – one advantage of this framework is that the number of clusters K does not need to be pre-determined by the practitioner. Yang et al. (2016) adapt the K -means algorithm to jointly perform market segmentation with response modeling, referring to their approach as *K-Classifiers Segmentation*. The algorithm starts with an initial assignment of observations to clusters, and iteratively (1) fits response models within each cluster, and (2) reassigns observations to the clusters whose response model best describes them (according to a given loss function). Both the methodology of Bernstein et al. (2018) and Yang et al. (2016) do not utilize customer attributes when performing market segmentation – the works assume that customers have already been pre-grouped into “customer classes” according to their demographic information, and the algorithms then map the customer classes to clusters. Baardman et al. (2017) use a similar approach to *K-Classifiers Segmentation* to simultaneously cluster products and fit sales forecasting models within each cluster. The authors propose retroactively fitting a classification machine learning model (e.g., logistic

regression) for mapping product features to the cluster assignments outputted by the K -Classifiers Segmentation method. In comparison to the aforementioned methods, the MST approach *directly* utilizes available contextual attributes when learning its market segmentation. Jagabathula et al. (2018b) propose a method for simultaneous market segmentation and response modeling which (1) fits a response model to the entire population of customers, and (2) segments customers according to how their response behavior differs from the population model (e.g., through a log-likelihood score). The approach does not segment customers on the basis of their demographic features, but rather on their observed historical response behavior. Therefore, their approach is specialized for personalizing recommendations to *returning* customers, whereas our approach may also be used for personalizing decisions to new customers (assuming that informative contextual attributes are readily available).

Regarding our IRT algorithm for bid landscape forecasting, building model trees with isotonic regression leaf models has not been proposed in the prior literature, and the idea of using isotonic regression to model auction dynamics is also novel. Wang et al. (2016) also propose a model tree approach for bid landscape forecasting, although their approach relies on second-highest bid prices being directly observable for auction win outcomes (i.e., second-price auction dynamics). In contrast, our model may be applied to first-price auctions in which the highest outside-bid prices are always unknown. Most major ad exchanges are anticipated to switch to first-price auctions by the end of 2019 (Sluis 2019). The approach in Wang et al. (2016) selects decision tree splits which attempt to maximize the KL-divergence of the bid landscape forecasting models within the resulting segments, and uses a heuristic procedure to do so. Conversely, the MST training algorithm selects splits which (individually) maximize the predictive accuracy of the resulting bid landscape forecasting models.

3. Methodology

3.1. Problem Formulation

We now provide a general formulation of a personalized decision-making problem, which we break down into three components. First, the agent observes variables x which serve as the *context* for the decision. The agent then makes a decision encoded by features p , and finally a user’s response y is observed as a result of the decision. We emphasize that our approach can handle categorical, ordinal, and continuous data with respect to x , p , and y . As examples of these components, for the choice prediction problem, the contextual variables x consist of features about the user (e.g., prior purchase history), the decisions p correspond to the options offered by the firm to the user (e.g., assortment of products), and the response y indicates which option the user chose. For the bid landscape forecasting problem, the contextual variables x encode the features describing the current user and auctioned ad spot (e.g., the ad spot’s width/height), the decision $p \geq 0$ is the firm’s submitted bid price, and the response $y \in \{0, 1\}$ indicates the outcome of the auction (win/loss).

Our objective is to build an interpretable model for personalized decision-making problems that accomplishes two goals:

1. **Market Segmentation.** Our model should yield an interpretable market segmentation of the contextual variables $x \in \mathcal{X} \subseteq \mathbb{R}^m$. Here, we define an interpretable market segmentation as a partition of the context space \mathcal{X} into a finite number of disjoint segments. Beyond interpretability, market segmentation allows us to fit simple response models for each market since the user features have already been accounted for in the segmentation. In contrast, one can avoid market segmentation and fit a single, high-dimensional model for personalization (with many interaction terms between contexts and decision variables), although this approach can be computationally challenging and less interpretable.

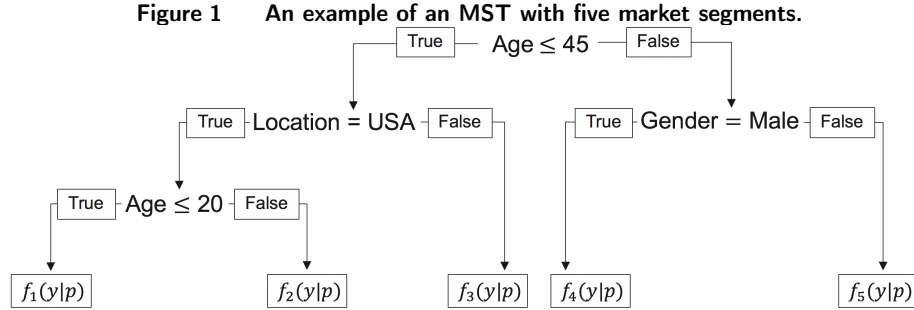
2. **Response Modeling.** Our model should accurately estimate the probability of each response y for all contexts x and decisions p , $\mathbb{P}(y|x, p)$. Note that for the bid landscape forecasting problem, $\mathbb{P}(y|x, p)$ yields the distribution (c.d.f.) of the highest outside bid price p_o , as $\mathbb{P}(y = \text{win}|x, p) = \mathbb{P}(p_o \leq p|x)$. Accurately estimating $\mathbb{P}(y|x, p)$ is a critical component for personalized decision-making, in which the goal is to prescribe personalized decisions p to contexts x which achieve the most favorable responses y .

Section 3.2 discusses our MST approach which tackles these tasks *jointly*, with the market segmentation being informed by the resultant response models. This arguably yields a more informative market segmentation – users in the same segment of the CMT can be interpreted as having similar choice behavior, and auctions in the same segment of the IRT can be interpreted as having similar bid landscapes. Section 3.3 presents an algorithm for training MSTs from historical data.

3.2. Market Segmentation Trees (MSTs)

We tackle the personalized decision-making problem using an approach we call *Market Segmentation Trees* (MSTs). MSTs perform market segmentation according to successive decision tree splits on the contextual variables x . Each split partitions the space of contexts with respect to a single contextual variable; continuous and ordinal contexts are split using inequalities (e.g., “Age ≤ 40 ?”), while categorical contexts are split using equalities (e.g., “Gender = Male?”). Each resulting market segment l – referred to as a *leaf* of the MST and defined solely by contextual variables x – contains a response model $f_l(y|p)$ estimating the distribution of the response y given the decision p for users in segment l . Since different market segments may exhibit different distributions of the response y , the response models $f_l(y|p)$ may vary significantly across segments.

To use the MST for prediction, i.e. to estimate $\mathbb{P}(y|x, p)$ for a given context x and decision p , one simply needs to follow the decision tree splits to the leaf l to which the context x belongs and output $f_l(y|p)$. For example, with respect to the MST in Figure 1, a user with context $x = \{\text{Age} =$



Note. Decision tree splits are performed with respect to the contextual variables *age* (numeric), *location* (categorical), and *gender* (categorical). Each of the resulting market segments contains a unique model $f_l(y|p)$ of the distribution of the response given the decision variables.

30, Location = USA, Gender = Male} would belong to segment $l = 2$, so response model $f_2(y|p)$ would be used to make predictions with respect to that user's response behavior.

As Figure 1 demonstrates, the market segmentation produced by an MST is interpretable and easily visualized. In high-dimensional settings too large to visualize, MSTs may still be viewed as interpretable as they map each context to a single, interpretable response model which may be easily analyzed for behavioral insights. Since the contextual variables are already accounted for in the MST's decision tree splits, the response models focus solely on the relationship between the decision variables and responses, allowing them to be simple and interpretable. MSTs also have a number of desirable properties as estimators. The decision tree splitting procedure is non-parametric, allowing MSTs to model potentially non-linear relationships in the mapping from contexts to segments. MSTs also naturally model interactions among the contextual variables; for example, in the MST in Figure 1, the variable *age* interacts with both *location* and *gender*.

MSTs provide a general framework that can be utilized to design new algorithms for various personalized decision-making problems. To do so, the practitioner simply needs to specify a family of response models for the given problem at hand, as well as a loss function for training the response models (see Section 3.3, where this notion is described in greater detail). As a proof of concept and to demonstrate the versatility of our methodology, we design from our MST framework two new algorithms for fundamental personalized decision-making problems, outlined in the two subsections below.

3.2.1 Choice Model Trees (CMTs)

We propose a specialized MST algorithm, *Choice Model Trees (CMTs)*, which can be used to predict a user's choice amongst multiple options. The CMT segments users on the basis of available demographic information (e.g., age or location) and activity history on the site (e.g., prior purchases or search queries). Within each segment, a Multinomial Logit (MNL) choice model is fit as the

response model to predict the probability that users in that market segment choose each option. MNL models are widely used for modeling user choice behavior, largely because the choice probabilities can be expressed in closed form and are therefore readily interpretable (Train 2009). Let $p = \{p_h\}_{h \in [H]}$ denote the collection of feature vectors encoding an offered assortment of H options, with $p_h \in \mathbb{R}^q$ representing the feature vector encoding option $h \in [H] := \{1, \dots, H\}$ in the assortment. If the options correspond to different products, for example, then the elements of p_h might include the products' price, color, and brand. Let $y \in \{0, 1, \dots, H\}$ denote the user's choice when being presented with the assortment p – specifically, let

$$y = \begin{cases} h, & \text{if the user chooses option } h \in [H], \\ 0, & \text{if the user does not choose any option.} \end{cases}$$

Each leaf l of the CMT contains an MNL instance, $f_l(y|p)$, estimating the probability of each outcome y given the features p describing the assortment of options. Let $\beta_l \in \mathbb{R}^q$ denote the parameters of the MNL model in leaf l . Then, the random utility that a user belonging to leaf l experiences by choosing option h is modeled as

$$U_h = \beta_l^T p_h + \epsilon_h,$$

where $\{\epsilon_h\}_{h \in [H]}$ are random (Gumbel-distributed) noise terms independently and identically distributed across options. Note that each component c of β_l , denoted by β_l^c , can be interpreted as the marginal utility increase the user experiences given a one-unit increase in the c -th option feature (e.g., product price). The user is assumed to be utility-maximizing, choosing option h over h' if $U_h > U_{h'}$, and choosing no option if none of the utilities are greater than a reference utility U_0 which can be set to $U_0 = 0$ without loss of generality (Train 2009). Thus, the probability of observing each choice can be shown to take the following form:

$$\begin{cases} f_l(y = h | p) = \frac{e^{\beta_l^T p_h}}{1 + \sum_{h' \in [H]} e^{\beta_l^T p_{h'}}}, \forall h \in [H] \\ f_l(y = 0 | p) = \frac{1}{1 + \sum_{h' \in [H]} e^{\beta_l^T p_{h'}}} \end{cases} \quad (1)$$

Note that the number of options in the assortment (H) is permitted to vary across users. Our work also accommodates a noteworthy alternate form of the MNL model which allows for *option-specific* parameters $\beta_{l,h}$, in which the utility from option h takes the form $U_h = \beta_{l,h}^T p_h + \epsilon_h$. The choice probabilities for this model can be derived in a similar manner as above.

3.2.2 Isotonic Regression Trees (IRTs)

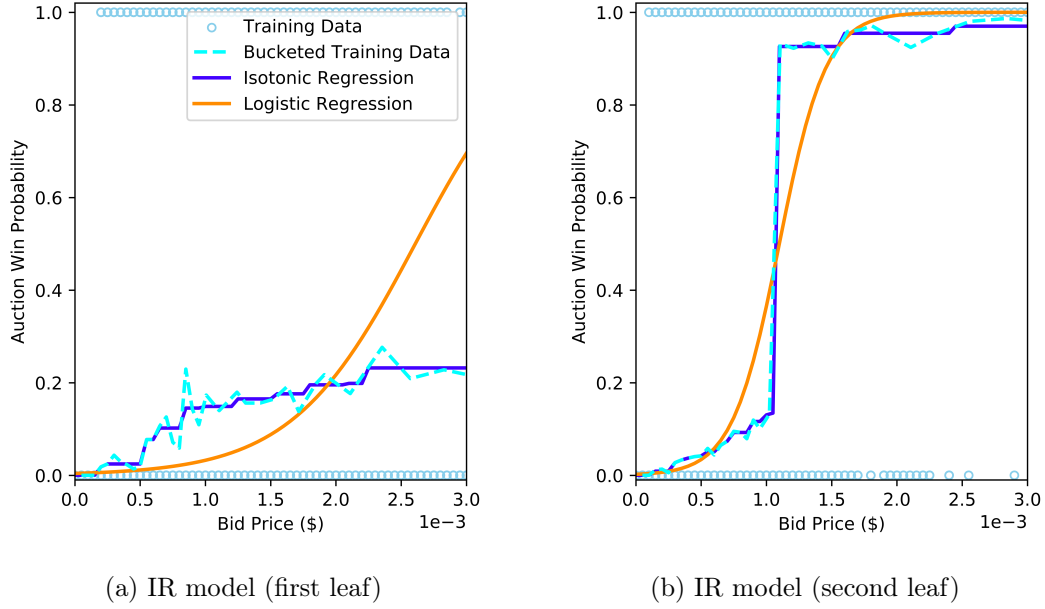
We propose a specialized MST algorithm, *Isotonic Regression Trees* (IRTs), which can be used to solve the bid landscape forecasting problem. The tree segments ad spot auctions according to contexts

such as the auctioned ad spot’s dimensions in pixels and the visiting user’s location. Here, an ad spot auction refers to the selling mechanism of a particular advertisement opportunity (e.g., location on website) for a particular user (e.g., visitor to website). Thus the “market” to be segmented in this application includes all instances of advertisement opportunities for users. Within each leaf of the tree, an isotonic regression model is used as the response model to estimate the bid landscape of the auctions belonging to that leaf. Let $p \geq 0$ denote an auction bid, and let y be a binary variable which equals 1 if and only if the bid won the auction. The isotonic regression model in each leaf l , denoted by $f_l(y|p)$, estimates the probability that a given bid of p will result in an outcome of y for auctions in that leaf.

An isotonic regression model is a free-form curve fitted to historical data in the following way: the curve is the best *monotonically-increasing* curve that minimizes the training set prediction error (as defined by mean-squared error). The constraint of monotonicity is natural for this application, as the probability of an auction win should increase when the submitted bid p increases. Isotonic regression models are non-parametric and uniformly consistent estimators, feasibly capturing any noisy, monotone function given sufficient data (Brunk 1970, Hanson et al. 1973). Also, the decision tree segmentation procedure of MSTs is non-parametric, imposing no distributional assumptions about the data. Thus, IRTs offer a fully non-parametric, interpretable algorithm for bid landscape estimation.

Figure 2 plots the estimated isotonic regression models in two different leaves of an IRT trained on historical bidding data collected by an anonymous DSP. As the figure demonstrates, different types of auctions can have differently-shaped bid landscapes, and the isotonic regression models are flexible enough to capture these differences. The figure also suggests that parametric models can fail to exhibit this level of robustness: a logistic regression model trained on the same data fails to adequately capture the (approximately) concave bid landscape shown in Figure 2a. Logistic regression is one of the most common parametric approaches for probabilistically modeling binary response data and has been used for personalized marketing in several previous works (McMahan et al. 2013, Chen et al. 2015, Etzl et al. 2019).

We mention in passing that IRTs also offer a powerful new tool for *personalized pricing*. In these settings, the contextual variables x are features encoding the visiting customer, the decision p is the price of the offered product, and the response y is a binary indicator of whether the customer purchased the product at that price. IRTs offer a non-parametric alternative for demand modeling which (1) naturally captures the monotonic (decreasing) relationship between product price and customer purchase probability through isotonic regression, and (2) finds an interpretable market segmentation driven by differences in customers’ demand models.

Figure 2 Estimated bid landscapes in two leaves of an IRT fit on bid data collected by a large DSP.

Note. The isotonic regression models are fit on training sets of auction outcomes (blue circles) within each leaf. Also included in the figures are logistic regression models trained on the same data. The models are compared against a curve (blue dashed line) constructed by bucketing the training set bids and computing the fraction of auction wins in each bucket.

3.3. Training Procedure

We present an algorithm for training the MSTs outlined in Section 3.2. Assume there are n training set observations, and denote the collection of all such observations by $[n] = \{1, \dots, n\}$. Let $i \in [n]$ denote an individual observation which consists of a context x_i , decision p_i , and response y_i . The training algorithm is fed the data $\{(x_i, p_i, y_i)\}_{i \in [n]}$ and learns (1) a segmentation of the contextual features x_i , and (2) the response models $f_i(y|p)$ within each segment. In Section 3.3.1, we first tackle problem (2) in isolation, showing how the final response models are optimized to accurately estimate the distributions of responses given decisions in each leaf. We then propose in Section 3.3.2 a training procedure for learning the market segmentation, which is driven by optimizing the accuracy of the resulting collection of response models. In Section 3.3.3, we discuss our open-source code base for training MSTs which includes several features such as parallel processing for improved computational tractability on high-dimensional datasets. Finally, to theoretically demonstrate the tractability of our training procedure, we analyze in Section 3.3.4 the asymptotic computational complexity of MST training in terms of the depth of the tree and number of contextual variables. In particular, we show that the parallel processing scheme implemented in our code base can significantly reduce or even nullify the effect of tree depth on computational complexity.

3.3.1 Learning the Response Models

In what follows, we denote by $S_l \subseteq [n]$ the subset of training set observations which belong to leaf l of the MST, and we designate by $f_l(y|p)$ the corresponding response model. Given a class \mathcal{F} of response models, the goal is to find the response model $f_l \in \mathcal{F}$ which most accurately models the data $\{(p_i, y_i)\}_{i \in S_l}$. Specifically, our notion of model accuracy is captured by a loss function $\ell(p_i, y_i; f_l)$ which penalizes discrepancies between the observed response y_i and the predicted response distribution $f_l(y|p_i)$. We assume that this loss function is *additive*, i.e. the loss incurred on the entire training data should be interpreted as the sum of the prediction losses for each individual observation. Consequently, each response model is trained by solving the following empirical risk minimization problem:

$$\mathcal{L}(S_l) := \min_{f_l \in \mathcal{F}} \sum_{i \in S_l} \ell(p_i, y_i; f_l) \quad (2)$$

To tailor our MST training algorithm to specific applications, the practitioner simply needs to specify a class of response models \mathcal{F} and a loss function $\ell(p_i, y_i; f_l)$ for evaluating models $f_l \in \mathcal{F}$. Below are examples for how these would be defined for the CMT and IRT models:

- *CMT*: The class of response models \mathcal{F} are the set of MNL choice models characterized by coefficients $\beta \in \mathbb{R}^q$ that satisfy Eq. (1). MNL models are typically trained using the loss function of negative log-likelihood, defined as $\ell(p_i, y_i; f_l) := -\log(f_l(y = y_i | p_i))$.
- *IRT*: Since the response y_i is binary, then without loss of generality we may identify \mathcal{F} as a class of functions $f_l(p)$ estimating the probability of $y = 1$ given the user belongs to segment (leaf) l . Isotonic regression fits a monotonically increasing function to the training data which minimizes mean squared error. Consequently, we define \mathcal{F} as the set of all monotonically-increasing functions $f_l: \mathbb{R} \rightarrow [0, 1]$, and the loss function is defined as $\ell(p_i, y_i; f_l) := (y_i - f_l(p_i))^2$.

3.3.2 Learning the Segmentation

We now describe our market segmentation algorithm. From Eq. (2), $\mathcal{L}(S_l)$ represents the total loss after training a response model on the collection of observations S_l . The goal of our market segmentation algorithm is to find the MST which segments the data into L leaves, S_1, \dots, S_L , whose response models collectively minimize training set loss:

$$\min_{(S_1, \dots, S_L) \in \mathcal{P}(n)} \sum_{l=1}^L \mathcal{L}(S_l), \quad (3)$$

where $\mathcal{P}(n)$ is the collection of partitions satisfying $\bigsqcup_l S_l = [n]$.

It is clear that this optimization problem is NP-Complete, since training optimal classification trees is a special case which is known to be NP-Complete (to formulate a classification tree as an MST, let each response model map to a constant $K \in \{0, 1\}$ and define the loss function as classification

loss) (Laurent and Rivest 1976). Thus, we rely on a technique known as *recursive partitioning* to approximate an optimal market segmentation. The procedure is directly analogous to the CART algorithm for greedily training classification trees, recursively finding the best decision-tree split with the smallest loss across the resulting leaves (Breiman et al. 1984).

Denote the j -th attribute of the i -th context by $x_{i,j}$. Starting with all of the data, consider a decision tree split (j, s) encoded by a splitting variable j and split point s which partitions the data into two leaves:

$$S_1(j, s) = \{i \in [n] \mid x_{i,j} \leq s\} \text{ and } S_2(j, s) = \{i \in [n] \mid x_{i,j} > s\},$$

if variable j is numeric, or

$$S_1(j, s) = \{i \in [n] \mid x_{i,j} = s\} \text{ and } S_2(j, s) = \{i \in [n] \mid x_{i,j} \neq s\},$$

if variable j is categorical (note that this is a slight abuse of notation, as $S_1(j, s)$ and $S_2(j, s)$ do not represent the *final* leaves of the tree but rather could eventually become internal splitting nodes as the training procedure progresses). We wish to find the decision tree split (j, s) resulting in the minimal loss incurred in leaves $S_1(j, s)$ and $S_2(j, s)$, which corresponds to the following optimization problem:

$$\min_{j,s} \mathcal{L}(S_1(j, s)) + \mathcal{L}(S_2(j, s)) \quad (4)$$

This problem can be solved through an exhaustive search over all potential splitting variables and split points, choosing the split (j, s) which achieves the best value of the objective function. When evaluating each split (j, s) , the data is partitioned according to the split and a response model is fit in each partition through solving Eq. (2); the training errors from these models are then summed together to compute objective function (4). For continuous numerical variables, a search over all possible split points may be computationally infeasible, so instead the following approximation is used. The values of the continuous variable observed in the training data are sorted, and every q th quantile is evaluated as a candidate split point, where q is a parameter chosen by the practitioner. In our numerical experiments, the value of q varies between 2 and 10 depending on the application.

After a split is selected in this manner, the procedure is then recursively applied in the resulting leaves until a stopping criteria is met. Examples of stopping criteria include a maximum tree depth limit or a minimum number of training set observations per leaf. To prevent overfitting, the CART pruning technique detailed in Breiman et al. (1984) can be applied to the MST using a held-out validation set of data. To keep our paper concise, we refer the reader to Breiman et al. (1984) for an in-depth description of the pruning method.

3.3.3 Code Base for Training MSTs

We provide an open-source implementation of our training procedure in Python (Aouad et al. [n. d.]). The implementation is general, allowing practitioners to specify the class of response models \mathcal{F} , loss function $\ell(p_i, y_i; f_l)$, and response model training procedure (i.e., procedure for solving Eq. (2)) which is best suited for their particular application. The stopping criteria used in training the MST is customizable as well: optional criteria include a maximum tree depth limit and a minimum number of observations per leaf.

Our code offers several features for improved scalability on high-dimensional datasets. First, we develop a *parallelization scheme* to be used by our algorithm in the event that multiple processor cores are available. The main computational bottleneck of the training algorithm is in repeatedly solving the split selection optimization problem of Eq. (4) to determine all internal splits of the MST. At a given depth of the MST, determining all splits at this depth can be thought of as independent subproblems which can be computed in parallel; thus, our parallelization strategy distributes all instances of the split selection optimization problem of Eq. (4) at a given tree depth across any available processor cores. This parallelization scheme can lead to a significant computational speedup of the training algorithm. We examine its impact on the training algorithm’s computational complexity in Section 3.3.4, and we show that the strategy can significantly reduce or even nullify the effect of tree depth on computational complexity for a sufficiently large number of training observations.

Second, we take advantage of *warm-starts* to reduce the number of gradient descent iterations needed to fit the response models as part of the split selection optimization problem of Eq. (4). Specifically, for a given split, the parameter estimates of the parent’s response model are provided as initial conditions for the gradient descent algorithm when fitting the response models of each of its children. Among all response models computed in the tree, parent nodes are arguably the most similar and informative estimates available. Moreover, this strategy evaluates and discards uninformative splits quickly, since in these cases the children’s response model parameters are likely to be very similar to those of their parent and therefore training them requires very few iterations when warm started with the parent’s coefficients. Notably, we also apply a special warm-starting procedure when finding the optimal split point for a numerical variable. Any candidate split points for the numerical variable are evaluated in order of magnitude (e.g., “ $x < 1$ ”, then “ $x < 2$ ”, then “ $x < 3$ ”, etc.), and the response models corresponding to a particular split point are warm started with those from the previous split point. We find that the warm-starts significantly reduce the overall computational cost associated with learning the response models as part of the training procedure.

Finally, our code supports an *adaptive optimization strategy* to fit the response models, which we describe below. As the recursive partitioning training procedure progresses, the number of response models in the tree increases and the average number of observations per response model therefore

decreases. Consequently, we observe empirically that different stages of the training procedure may require different response model optimization algorithms, adapted to the number of observations at hand. At the beginning of the recursive partitioning procedure, response models are fit to large subsets of the training set. On such large training sets, optimization algorithms that use mini-batching (e.g., stochastic gradient descent) may be required to efficiently fit the response models. However, as the recursion progresses and the tree depth increases, the computational burden shifts to fitting many small response models quickly, and thus, optimization methods with few gradient descent iterations like Newton’s method are more efficient. Our code supports adapting the response model optimization algorithm used during the fitting process to the current number of observations. In our implementation of the CMT’s training algorithm, we shift from stochastic gradient descent to Newton’s method to fit the response models as the training procedure progresses.

3.3.4 Computational Complexity

We provide theoretical bounds for the computational complexity of the MST training procedure as the number of training set observations becomes large. For ease of analysis, we assume throughout this section that the contextual variables are all binary and that the tree is trained to a fixed depth specified a priori by the practitioner. Let n denote the number of training set observations, m denote the number of contextual variables, and D denote the depth of the MST being trained. We demonstrate two key properties, under some mild assumptions, of our training algorithm which illustrate its scalability to high-dimensional datasets:

1. The training algorithm’s computational complexity is equivalent to fitting $O(D \cdot m)$ response models on training data of size n (see Theorem 1).
2. Let Q denote the number of cores available for parallel processing, and assume that the tree splits selected by the training algorithm are reasonably balanced. Then, the training algorithm’s computational complexity is equivalent to fitting $O(\max\{D/Q, 1\} \cdot m)$ response models on training data of size n (see Theorem 2).

Given that the number of response models in the MST scales exponentially in the tree’s depth, one might expect the training algorithm’s computational complexity to be exponential in D . However, we show through property (1) that under reasonable technical assumptions, training time scales linearly in tree depth and in the number of contextual variables. Moreover, property (2) implies that if the algorithm has access to a sufficiently large number of cores for parallel processing, i.e. if Q is close in magnitude to D , then the effect of tree depth on training time can be greatly diminished or even nullified. Typically, compute nodes on high-performance computing clusters have at least 24 cores available for submitted jobs, and for many applications it is reasonable to expect MST depth to be less than 24.

We now present two theorems which formally express the above properties. Let r denote the number of parameters to be learned in the response models. Note that r is implicitly related to the dimension of the decision variables p and the response variables y . Let $f(n, r)$ denote the computational cost of fitting a response model with r parameters to training data of size n , i.e. the cost of solving the optimization problem in Eq. (2). For a given internal MST depth $d \leq D$, number the nodes at depth d according to $\{1, \dots, 2^d\}$. Let $N_{\mathcal{T}}(d, l; n)$ denote the number of training set observations belonging to node $l \in \{1, \dots, 2^d\}$ at depth d of MST \mathcal{T} . Note that $N_{\mathcal{T}}(D, l; n)$ may be interpreted as the number of observations belonging to each leaf l of the MST \mathcal{T} (as by definition all leaves are of depth D in the MST).

Our first theorem relies on the following technical assumptions (the formal definitions for any big- O notation are provided in Sections A and B of the appendix):

ASSUMPTION 1. $f(n, r) = O(g(n, r))$.

ASSUMPTION 2. $g(n, r)$ is continuous, monotonic nondecreasing, and convex in n for all $n \geq 0$.

ASSUMPTION 3. $N_{\mathcal{T}}(D, l; n) \rightarrow \infty$ as $n \rightarrow \infty$ for all l and \mathcal{T} .

ASSUMPTION 4. $g(n, r) \rightarrow \infty$ as $n \rightarrow \infty$.

Assumptions 1 and 2 express that $f(n, r)$ can be asymptotically bounded by another function $g(n, r)$ which is continuous, monotonic non-decreasing, and convex in n . For example, if $f(n, r)$ denotes the training time of a linear regression response model on n observations and r parameters, then we may set $g(n, r) = nr^2 + r^3$ (the complexity of computing the closed-form Ordinary Least Squares estimate) which satisfies the functional properties of Assumptions 1 and 2. Assumption 3 may be interpreted as a weak assumption on the distribution of the contextual variables in the training set. The assumption expresses that, for every finite partitioning of the contextual variables dictated by different MSTs of depth D , the number of observations in each partition increases without bound as n increases. Finally, Assumption 4 ensures that $g(n, r)$ is an asymptotically unbounded function of n . This property holds for any non-constant runtime function, including the function $g(n, r) = nr^2 + r^3$ specified above.

Having defined the requisite assumptions, we now present our first theorem:

THEOREM 1. *If assumptions 1, 2, 3, and 4 hold, then the computational complexity of the MST's training algorithm may be expressed as $O(D \cdot m \cdot g(n, r))$.*

The proof of the theorem is contained in Appendix A. Theorem 1 implies that the complexity of the MST's training algorithm is equivalent to fitting $C \cdot D \cdot m$ response models to the training data, where C is a constant independent of the problem parameters. We demonstrate in the appendix that for sufficiently large n , C may be bounded by $(1 + \epsilon)$ where ϵ is taken to be arbitrarily small.

Next, we analyze how the computational complexity of the training procedure is improved through use of the parallel processing scheme outlined in Section 3.3.3. For depths $d = 0, 1, \dots, D - 1$, the training algorithm parallelizes the split selection procedure of Eq. (4) across all nodes of depth d within the MST. Note that all nodes across a given depth d collectively partition the training set observations, i.e. $\sum_l N_{\mathcal{T}}(d, l; n) = n$. In order to effectively distribute each node's workload across the available cores for parallel processing, it is important that the partitioning of observations across nodes is not greatly imbalanced. Indeed, the worst case for parallel processing is for one node to contain all of the observations, in which case parallelization yields no benefits for our training algorithm. Thus, we assume that all splits chosen by the recursive partitioning procedure are reasonably balanced, i.e. partition the data into roughly equal proportions. This condition gives rise to the following additional technical assumptions for our next theorem:

ASSUMPTION 5. *Let \mathcal{T} denote the trained MST. For all $d \in \{0, \dots, D - 1\}$ and $l \in \{1, \dots, 2^d\}$, $N_{\mathcal{T}}(d, l; n) = O(n/2^d)$.*

ASSUMPTION 6. *For any constant C , $g(Cn, r) = O(g(n, r))$.*

Assumption 5 states that all splits in the trained MST partition the observations into roughly equal proportions up to a multiplicative constant. To ensure this assumption holds in practice, one may restrict the split selection procedure of Eq. (4) to only include splits which are not greatly imbalanced. This is arguably desirable from a learning perspective as well, as balanced splits can yield shallower and thus more interpretable decision trees. Assumption 6 is a technical assumption which is needed for the following chain of inequalities combining Assumptions 1, 2, 3, 5, and 6 to hold. Let \mathcal{T} denote the trained MST, then for all $d \leq D - 1$, $l \in \{1, \dots, 2^d\}$, and n sufficiently large,

$$\begin{aligned} f(N_{\mathcal{T}}(d, l; n), r) &\leq C_1 g(N_{\mathcal{T}}(d, l; n), r) \\ &\leq C_1 g(C_2 n / 2^d, r) \\ &\leq C_1 C_3 g(n / 2^d, r), \end{aligned}$$

where C_1 , C_2 , and C_3 are universal constants. These inequalities together express that $f(N_{\mathcal{T}}(d, l; n), r) = O(g(n/2^d, r))$, where the first inequality uses Assumptions 1 and 3, the second inequality uses Assumption 5 and monotonicity of $g(n, \cdot, \cdot)$, and the third inequality uses Assumption 6. Many runtime functions satisfy Assumption 6, including the complexity of computing the linear regression OLS estimator and, more generally, any function polynomial in n . For example, if $g(n, r) = n^a h(r)$, then:

$$g(Cn, r) = C^a n^a h(r) = C^a g(n, r) = O(g(n, r))$$

Having motivated Assumptions 5 and 6, we now present our second theorem.

THEOREM 2. *If assumptions 1, 2, 3, 4, 5, and 6 hold, then the computational complexity of the MST’s training algorithm with parallel processing may be expressed as $O(\max\{D/Q, 1\}mg(n, r))$.*

The proof of the theorem is given in Appendix B. Theorem 2 implies that the computational complexity of the training procedure is equivalent to fitting $O(\max\{D/Q, 1\}m)$ response models to the training data. As discussed previously, we may diminish or even nullify the effect of tree depth on model complexity by setting $Q \approx D$, which is often feasible in practice due to the large number of cores available on high-performance computing clusters.

4. Experimental Results

In this section, we evaluate the empirical performance of our Market Segmentation Tree methodology on several datasets. Our results demonstrate that Market Segmentation Trees are not only interpretable models but also yield competitive predictive performance of response behaviors when compared with other state-of-the-art approaches.

4.1. Choice Model Tree Performance Evaluation

First, we apply the CMT algorithm to datasets derived from three “ground truth” models, each using a different method for simulating choice behavior. Second, we train and evaluate CMTs on hotel search data from the travel booking website Expedia.

4.1.1 Experiments Using Synthetic Datasets

Dataset Generation. In each dataset, a user is encoded through four contextual variables (x) which can be used for the purposes of market segmentation. Each user is shown a random assortment (p) of 2-5 options, with each option encoded by four features (e.g., price). The user’s response (y) to the assortment represents which option the user chose. The objective is to find a market segmentation of the contextual variables which leads to accurately predicting choice probabilities.

We generate 10 datasets – including contexts, assortments, and choices – from each of three different “ground truth” models, summarized below. Further details of how each dataset is generated are included in Appendix C. Each dataset is comprised of 25000 training set observations, 25000 validation set observations, and 25000 test set observations.

1. “Context-Free” MNL: A single MNL model is used to simulate choices for all users. Contextual variables are simulated independently from choices, and therefore the contexts have no relevance to choice prediction. Note that this simple MNL ground truth corresponds to a CMT ground truth model of depth zero.

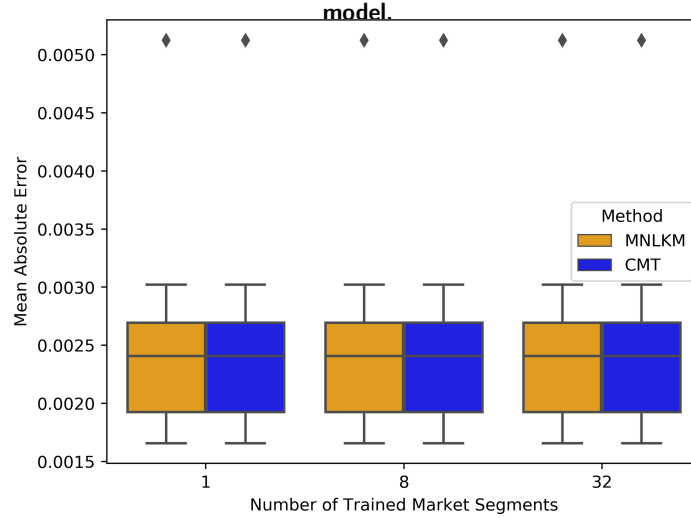
2. Choice Model Tree: Choices are simulated through a Choice Model Tree of depth 3. The CMT maps users to leaves through decision tree splits on the users’ contextual variables. Each leaf contains an MNL model used to simulate choices for all users belonging to that leaf.

3. *K*-Means Clustering Model: Choices are simulated according to the following procedure motivated by the popular *K*-means clustering market segmentation algorithm. Users belong to one of K market segments, where K is sampled from the possible values of $\{4, 5, 6, 7\}$. Each segment $k \in \{1, \dots, K\}$ is associated with its own MNL model as well as a “mean context vector” \bar{x}_k . Each observation in the dataset is simulated by (1) sampling a market segment k for the user, (2) sampling the user’s context (x) from a multivariate normal distribution with mean parameter \bar{x}_k , and (3) sampling the user’s choice (y) from segment k ’s MNL model.

Experimental setup. Using the training set observations for each of the generated datasets, CMTs are trained to depths of 0, 3, and 5, which correspond to 1, 8, and 32 leaves (i.e., market segments), respectively, and we prune the trees using the validation set observations according to the procedure described in Breiman et al. (1984). Recall that the CMT of depth 0 is equivalent to a single, context-free MNL model. We include CMTs of different depth sizes to examine the relationship between CMT model complexity and predictive accuracy. We also implement a *K*-means approach (MNLKM) that uses training set observations to first perform *K*-means clustering on the contextual features (x) and then fit an MNL model within each cluster. This clustering method represents a typical approach for market segmentation, whereby users are segmented based on feature dissimilarity rather than differences in their choice behavior. The number of clusters K is tuned on a grid of values $\{1, 2, \dots, K_{max}\}$ using the validation set observations. For each of the CMT depths we consider, we allow MNLKM to utilize up to the same number of market segments as that CMT; for example, a CMT trained to a depth of 3 is compared against an MNLKM utilizing at most $K_{max} = 2^3 = 8$ clusters. For further background on *K*-means clustering methods, we refer the reader to Friedman et al. (2001).

Predictive accuracy on the test set observations is measured using *mean absolute error* (MAE), which we define as follows. The *absolute error* with respect to a single observation is defined as the average, taken over all options in the offered assortment, of absolute differences between each option’s choice probability estimate and its *true* choice probability specified by the ground truth model. Next, the mean absolute error (MAE) is defined as the average absolute error over all observations in the test set.

Results. We first evaluate the CMT and MNLKM algorithms on 10 different datasets generated under the context-free MNL ground truth model in order to assess whether these approaches overfit on the contextual variables when they have no underlying relationship with the choice outcomes. The prediction errors incurred by the algorithms on the test sets are visualized in Figure 3. As might be expected, we observe that the performance of the CMT and MNLKM algorithms are equal when trained using a single market segment. Indeed, both a CMT of depth 0 and an MNLKM with $K = 1$ equivalently represent a single context-free MNL model. Since the ground truth for these datasets is

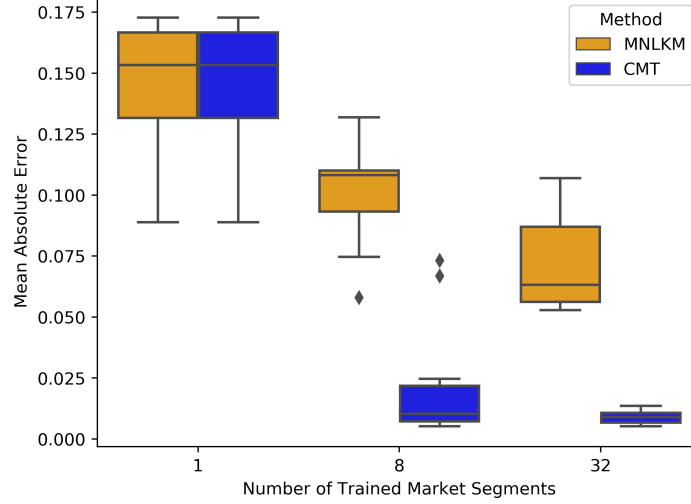
Figure 3 Test set MAEs incurred by the MNLKM and CMT algorithms on the context-free MNL ground truth

Note. Each boxplot is constructed from the 10 datasets generated from the context-free MNL ground truth model.

also a context-free MNL model, there is no model misspecification under both approaches. Hence, the two algorithms achieve high levels of accuracy with average MAEs of less than 0.0025.

When the CMT and MNLKM algorithms are trained on these datasets using a larger number of market segments, they run the risk of overfitting since there is no underlying relationship between contexts and choices specified by the context-free ground truth model. Overfitting could potentially lead to poor out-of-sample predictive performance as well as impair the overall interpretability of the models. However, we observe that the CMT and MNLKM algorithms achieve consistent test-set performance when permitted to utilize larger numbers of market segments. This signifies that the methodology used to prevent overfitting is working properly – the CMT pruning algorithm always prunes the tree to depth 0 across the 10 datasets, and the MNLKM algorithm always selects $K = 1$ through its tuning procedure.

We next evaluate the CMT and MNLKM algorithms on 10 different datasets generated under the choice model tree ground truth model in order to assess whether CMTs are able to accurately recover the ground truth when presented with a sufficient number of training observations and to examine how MNLKM performs under model misspecification. The prediction errors incurred by the algorithms on the test sets are visualized in Figure 4. When the CMTs are trained to a depth of 3 (with 8 market segments), they often – but not always – recover the choice probability distributions. Recall that the CMT ground truths have a depth of at most 3. Therefore, since our CMT algorithm trained to depth 3 does not always capture the behavior of the ground truth model even under a large number of training observations, we conclude that our training algorithm is not guaranteed to recover an “optimal” tree (namely, a tree that best fits the training data at a fixed tree depth). This is not surprising since our training method is based on a greedy recursive partitioning heuristic,

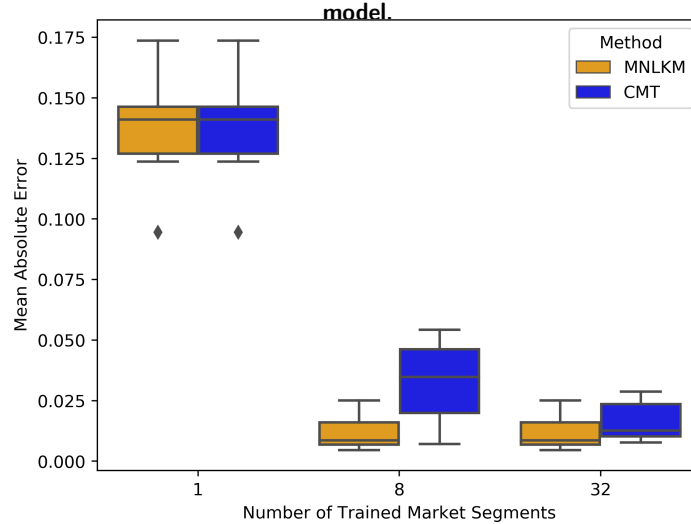
Figure 4 Test set MAEs incurred by the MNLKM and CMT algorithms on the CMT ground truth model.

Note. Each boxplot is constructed from the 10 datasets generated from the CMT ground truth model.

which comes with no guarantee for optimal recovery. Nevertheless, we observe that when the CMTs are trained to a large enough depth of 5, they are able to capture the choice probability distributions specified by the ground truth models almost perfectly. Although the combination of CMT splits found by the training algorithm is not necessarily optimal, each split is still selected to greedily minimize choice prediction error, and therefore when applied in succession the CMT will eventually estimate the underlying choice probability distributions to a very high degree of accuracy.

We also examine the performance of the MNLKM algorithm on the same datasets. Although the market segmentations obtained by MNLKMs improve prediction accuracy over the context-free models (i.e., $K = 1$), they fail to attain competitive performance relative to the CMT models. This is not necessarily surprising, since the ground truth is itself an instance of the CMT model, and therefore we naturally expect CMTs to outperform other models on such datasets. However, the degree of outperformance is rather large, with MNLKM incurring roughly 8 times the average MAE attained by the CMT models when the algorithms are trained using 32 market segments. These findings demonstrate that MNLKM is not necessarily robust to model misspecification. This is likely because MNLKM does not consider the accuracy of the resulting collection of choice models when performing market segmentation; instead users are clustered solely on the basis of similarities in their contextual features.

Finally, we evaluate the CMT and MNLKM algorithms on 10 different datasets generated under the K -means clustering ground truth model in order to assess whether our CMT algorithm can accurately model choice behavior even when choices are generated through ground truth models other than CMTs. The prediction errors incurred by the algorithms on the test sets are visualized in Figure 5. We first observe that MNLKM accurately recovers the response probability distributions specified

Figure 5 Test set MAEs incurred by the MNLKM and CMT algorithms on the K -means clustering ground truth

Note. Each boxplot is constructed from the 10 datasets generated from the K -means clustering ground truth model.

by the ground truth model when the number of clusters K is suitably large. However, we also observe that the CMT attains competitive predictive performance when trained to a suitably large depth of 5 (with the same number of leaves as K used in MNLKM). The CMT is therefore able to overcome the potential model misspecification introduced by the K -means clustering ground truth model. The CMT’s robustness to model misspecification may be explained in part by its nonparametric decision tree splits, which permit the CMT to flexibly capture highly irregular mappings from contexts to market segments. Also, as explained in the previous section, the CMT training algorithm is designed to yield a market segmentation which attains high choice prediction accuracy.

Overall, our experiments on the synthetic datasets demonstrate that CMTs reliably find market segmentations which accurately model choice behavior. We observe on the context-free MNL ground truth datasets that CMTs are robust to overfitting, and we observe on the CMT and K -means clustering ground truth datasets that our CMT training procedure reliably estimates the underlying choice probability distributions even when faced with potential model misspecification.

4.1.2 Experiment Using Expedia Hotel Booking Dataset

To supplement our synthetic data experiments in the previous section, we next evaluate CMTs on an actual dataset of hotel searches on Expedia made publicly available through the competition “Personalize Expedia Hotel Searches” hosted by ICDM in 2013 (ICDM 2013). Each hotel search instance consists of the following types of information: (1) features encoding the user and their search query (x), (2) the assortment of hotels displayed to the user including the display order on the search results page (p), and (3) a hotel booking (choice), if any, the user made in response to the displayed assortment (y). The CMT segments Expedia users on the basis of their user and search

query features, and within each segment the CMT applies an MNL to model user booking behavior as a function of their displayed hotel assortments. A more detailed description of the Expedia hotel booking dataset and minor pre-processing steps are included in Section C of the appendix. We randomly partition the observations (hotel searches) in the dataset into 239,490 training set observations, 79,831 validation set observations, and 79,831 test set observations.

Experimental setup. Similar to the experiments we ran using synthetic datasets, we evaluate the performance of our CMT algorithm compared to the context-free MNL and MNLKM benchmarks. We train our CMT algorithm using the training set observations and use the validation set observations to prune the tree according to the procedure described in Breiman et al. (1984). For the context-free MNL benchmark (MNL, for short), we use the training and validation set observations to fit a single MNL model that ignores any user and search contextual information (x); recall that this benchmark is equivalent to a CMT of depth 0. For the MNLKM benchmark, we use the training set observations to perform K -means clustering on the user and search features (x) and then fit an MNL model within each cluster; the number of clusters K is tuned using the validation set observations.

Predictive accuracy on the test set observations is measured using mean squared error (MSE), which we define as follows. The *squared error* with respect to a single search is defined as the sum, taken over all hotels in the displayed assortment, of squared differences between each hotel’s booking probability estimate and its realized 0/1 booking outcome; the no-booking event and its corresponding probability estimate are included in this sum as well. Mean squared error is then defined as the average squared error over all searches in the test set. This metric is also referred to in the literature as the *Brier score* and is a proper scoring rule for evaluating probabilistic predictions. We also report the average test set log-likelihood losses achieved by the CMT and benchmarks in our results. To ensure that the observed results are significant, we repeat the analysis across 10 different random allocations (“samplings”) of observations to the training, validation, and test sets.

We performed our numerical experiments on a Dell PowerEdge M915 Linux server using 75000 MB of memory and 8 processor cores. The CMT was trained using our open-source Python implementation with a minimum leaf size of 100 observations, and to create a tree which is easily visualized we restricted the maximum trained depth size to 8. We specify the negative log likelihood loss function from Section 3.3.1 to score hotel booking prediction error, while our pruning method is executed using the MSE metric. The training algorithm terminated after 18-28 hours of computational time across the 10 different samplings of the dataset. The CMT was then pruned on a validation set terminating after 2-4 minutes for each sampling. After pruning, the CMTs across the different samplings all had a maximal depth of 8 and contained between 74 and 100 leaves.

Table 1 Test set mean squared errors (MSEs) and log likelihoods of the CMT and the benchmarks on 10 different samplings of the dataset, labeled as S1 through S10.

(a) Test set MSEs

Model	S1	S2	S3	S4	S5	S6	S7	S8	S9	S10	Avg.	% Imp.
CMT	0.8304	0.8326	0.8313	0.8331	0.8335	0.8311	0.8315	0.8320	0.8308	0.8308	0.8317	
MNL	0.8489	0.8512	0.8505	0.8522	0.8519	0.8503	0.8499	0.8513	0.8496	0.8503	0.8506	2.2%
MNLKM	0.8345	0.8367	0.8357	0.8378	0.8380	0.8349	0.8356	0.8366	0.8355	0.8357	0.8361	0.53%

(b) Test set Log Likelihoods

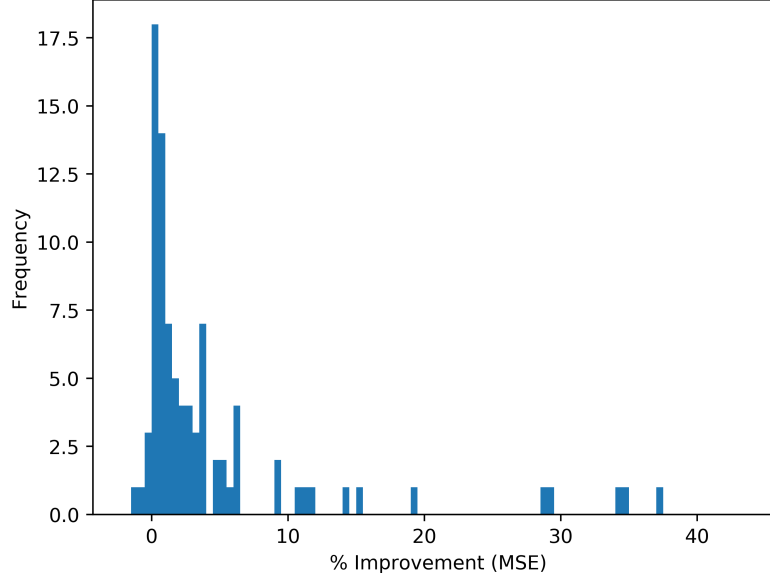
Model	S1	S2	S3	S4	S5	S6	S7	S8	S9	S10	Avg.	% Imp.
CMT	2.4038	2.4069	2.4052	2.4086	2.4119	2.4046	2.4033	2.4095	2.4051	2.4018	2.4060	
MNL	2.4439	2.4493	2.4467	2.4519	2.4533	2.4474	2.4448	2.4534	2.4472	2.4448	2.4483	1.72%
MNLKM	2.4119	2.4168	2.4138	2.4199	2.4217	2.4129	2.4124	2.4205	2.4160	2.4131	2.4159	0.41%

Note. The column “Avg.” measures the average error across all 10 samplings, and the column “% Imp.” measures the percentage improvement (decrease) in error from the CMT relative to each benchmark.

Results. The test set performance of the CMT and benchmarks across the 10 samplings is given in Table 1. In interpreting the reported MSEs, it is important to note that the highest possible squared error per search is 2 rather than 1 as one might expect; to see this, note that an error of 2 occurs when an incorrect outcome is predicted with probability 1. The CMT achieves higher test set accuracy than the MNL and MNLKM benchmarks across all 10 samplings of the dataset, which demonstrates the CMT’s *consistently* dominant performance over these algorithms. However, the magnitude by which the CMT outperforms the benchmarks is rather modest, with an average 2.2% MSE improvement over the MNL benchmark and 0.53% MSE improvement over MNLKM. One could argue that the small difference in performance between the context-free MNL and CMT signifies that market segmentation offers little predictive value for this dataset. However, as we next demonstrate, there exist “high-impact” market segments in which the CMT achieves substantial accuracy improvement over the MNL. Moreover, the CMT offers an easily interpretable segmentation unlike the other benchmarks.

Figure 6 provides a histogram of the CMT’s test set percentage improvement in MSE over the context-free MNL across the individual market segments (“leaves”) of the CMT; only markets with greater than 50 test set observations are included in the histogram. As the figure demonstrates, there exist several markets in which the CMT substantially outperforms the context-free MNL, with five markets seeing a 29-37% improvement in predictive accuracy. However, these markets are small in size, collectively comprising less than 2% of all test set observations; thus, they are largely neglected in the reported accuracy metrics. Moreover, the CMT achieves remarkably consistent improvement in accuracy over the MNL model across the 89 market segments included in the histogram – only five markets observe a loss in predictive performance, and the performance loss never exceeds -1.5%.

Figure 6 Histogram plotting the percentage improvements in test-set MSE of the CMT over the MNL benchmark across individual market segments (“leaves”) of the CMT.



Note. The data plotted in the histogram is from the first sampling S1; other samplings exhibit a similar shape.

Finally, the consistent outperformance of the CMT relative to MNLKM across the 10 samplings of the dataset illustrates the value of more informed market segmentation procedures in modeling and predicting user behavior. It is also important to note that the CMT achieves accuracy improvement over MNLKM while also being a more interpretable and easily visualized market segmentation model. While the magnitude of the CMT’s percentage improvement over MNLKM is modest at 0.53%, this can largely be explained by the small performance gain of the CMT over MNL explored above, as the MNL’s performance serves as a lower bound for MNLKM’s (noting that the MNL model is equivalent to an MNLKM model with $K = 1$). Therefore, we would expect to see even greater improvement in settings with more user features and whose user features better predict user choices.

4.2. Isotonic Regression Tree Performance Evaluation

In this section, we train and evaluate IRTs on bidding data from a Demand Side Platform (DSP), which will remain anonymous for confidentiality. The DSP provided us with several weeks of bidding data across three different ad exchanges. For each ad exchange (referred to as exchanges 1, 2, and 3), an IRT is trained on a dataset of historical bids submitted by the DSP between 1/13/2019 and 1/24/2019, which amount to a training set of 60-370 million bids per exchange. The IRT is pruned using a validation set holding out 15% of the training data. Finally, the IRT is evaluated on test sets of bids submitted between 1/25/2019 and 1/31/2019 amounting to 40-160 million bids per exchange. Each observation in the data is encoded by (1) the user and ad spot auction features available to the bidder (x), (2) the submitted bid price (p), and (3) the auction outcome (win/loss) (y). The IRT segments advertisement opportunities for users on the basis of user and ad spot auction features,

and within each segment the IRT applies an isotonic regression model to predict the auction win rate as a function of bid price. A detailed description of the user and ad spot auction features is included in Section C of the appendix.

Experimental setup. We train our IRT algorithm using the training set observations and use the validation set observations to prune the tree according to the procedure described in Breiman et al. (1984). We compare the IRT algorithm’s predictive performance with the following benchmarks trained and tested on the same datasets. In selecting which benchmarks to test alongside the IRT, we restrict our consideration to models which perform market segmentation and produce monotonically-increasing bid landscape curves.

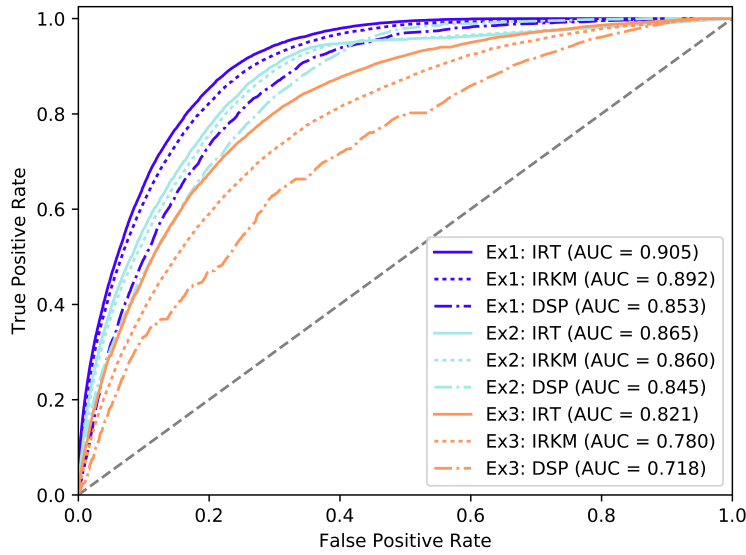
- *Const*: A model which predicts a constant win probability for all bid prices equal to the average training set win rate.
- *IR*: An isotonic regression model fit on the entire training set to estimate the auction win rate given the submitted bid price. This is a “context-free” model and does not incorporate the auction features (x).
- *IRKM*: Performs K -means clustering on the auction features (x) and then fits an isotonic regression model within each cluster; the number of clusters K is tuned using the validation set observations. K -means clustering is a common approach for market segmentation; this benchmark segments auctions based on feature dissimilarity rather than differences in their estimated bid landscapes.
- *DSP*: The bid landscape forecasting model which the DSP used in production during the testing period (1/25/2019-1/31/2019), which was also trained using the same data as our training set.
- *LRT*, *LR*, *LRKM*: We include analogous benchmarks testing the impact of using logistic regression models as opposed to isotonic regression models. Logistic regression is one of the most common parametric approaches for probabilistically modeling binary response data and has been used for personalized marketing in several previous works (McMahan et al. 2013, Chen et al. 2015, Etzl et al. 2019). The benchmark LR fits a single, “context-free” logistic regression model to the entire data; the benchmark LRKM performs K -means clustering on the auction features and fits a logistic regression model in each cluster; and the benchmark LRT runs our MST algorithm with logistic regression leaf models.

We conducted our experiments on a Dell PowerEdge M915 Linux server using 50000 MB of memory and 8 processor cores. The IRT was trained on each exchange separately using our open-source Python implementation, specifying a minimum leaf size of 10000 observations and no depth limit. The IRT was trained and pruned using the mean-squared-error (MSE) metric, which measures the average squared difference between the algorithms’ win probability estimates and the realized auction outcomes. The training procedure terminated after 12-35 hours of computational time across the

three exchanges. Next, the trees were pruned on a validation set, taking 6-35 minutes to complete per exchange. The final IRTs were of depths 52-78 and contained 800-4100 leaves. Although the IRTs for this application are too large to be visualized, they may still be regarded as interpretable bid landscape forecasting models since they map each auction to a single bid curve that can be easily visualized and analyzed for bidding insights. The reasonable computation times of our training and pruning procedures illustrate the scalability of our implementation when presented with large-scale high-dimensional data.

Results. The test set performance of the IRT and benchmarks for each ad exchange is given in Table 2, in which we report (1) overall MSE measured across the entire test data, and (2) the MSEs for each individual day of test data (1/25/19-1/31/19). The algorithms were also compared on the basis of their test-set ROC curves using the AUC (area under curve) metric. The ROCs and AUCs obtained by the algorithms are described by Figure 7.

Figure 7 Test set ROC curves and AUCs of our algorithm (IRT) and the benchmarks on three ad exchanges.



Note. The benchmark IR, not shown in the figure due to space constraints, achieved AUCs of 0.844, 0.776, and 0.716 on exchanges 1, 2, and 3, respectively.

The IRT attains a lower MSE than all benchmarks for each of the 21 individual days of test data. The IRT achieves a 5-29% improvement in overall MSE and 2-14% improvement in AUC over the DSP's approach across the three exchanges. The IRT also achieves a 7-13%/7-15% improvement in MSE/AUC relative to the IR benchmark and a 1-7%/0.6-5% improvement relative to IRKM. The strong performance of IRT over IR demonstrates the value of segmentation in bid landscape forecasting. Moreover, the superior performance of IRT over IRKM illustrates the gains achieved by applying a supervised segmentation procedure, driven by accurately capturing differences in the

Table 2 Test set mean squared errors (MSEs) of our algorithm (IRT) and the benchmarks on three ad exchanges.

(a) Test set MSEs: Exchange 1									
Model	1/25	1/26	1/27	1/28	1/29	1/30	1/31	Avg.	% Imp.
IRT	0.0465	0.0476	0.0432	0.0474	0.0482	0.0539	0.0482	0.0480	
LRT	0.0508	0.0508	0.0458	0.0504	0.0523	0.0588	0.0521	0.0518	7.3%
Const	0.0613	0.0613	0.0552	0.0599	0.0626	0.0718	0.0631	0.0625	23%
IR	0.0538	0.0545	0.0492	0.0529	0.0540	0.0619	0.0550	0.0546	12%
LR	0.0586	0.0584	0.0526	0.0571	0.0590	0.0680	0.0597	0.0593	19%
IRKM	0.0489	0.0497	0.0446	0.0488	0.0494	0.0556	0.0497	0.0497	3.4%
LRKM	0.0535	0.0540	0.0478	0.0522	0.0536	0.0603	0.0536	0.0537	11%
DSP	0.0564	0.0558	0.0508	0.0560	0.0569	0.0640	0.0592	0.0572	16%
(b) Test set MSEs: Exchange 2									
Model	1/25	1/26	1/27	1/28	1/29	1/30	1/31	Avg.	% Imp.
IRT	0.0276	0.0253	0.0341	0.0318	0.0366	0.0419	0.0405	0.0339	
LRT	0.0301	0.0273	0.0368	0.0344	0.0393	0.0450	0.0437	0.0366	7.3%
Const	0.0316	0.0285	0.0391	0.0364	0.0414	0.0471	0.0451	0.0384	12%
IR	0.0305	0.0275	0.0371	0.0349	0.0397	0.0449	0.0432	0.0368	7.9%
LR	0.0320	0.0287	0.0394	0.0366	0.0417	0.0473	0.0455	0.0387	12%
IRKM	0.0281	0.0258	0.0345	0.0321	0.0369	0.0423	0.0408	0.0343	1.2%
LRKM	0.0306	0.0278	0.0372	0.0347	0.0396	0.0453	0.0440	0.0370	8.4%
DSP	0.0296	0.0285	0.0377	0.0341	0.0379	0.0428	0.0416	0.0359	5.6%
(c) Test set MSEs: Exchange 3									
Model	1/25	1/26	1/27	1/28	1/29	1/30	1/31	Avg.	% Imp.
IRT	0.1200	0.1090	0.1098	0.1184	0.1230	0.1311	0.1268	0.1199	
LRT	0.1375	0.1198	0.1203	0.1303	0.1347	0.1386	0.1347	0.1310	8.5%
Const	0.1591	0.1361	0.1422	0.1510	0.1521	0.1631	0.1587	0.1520	21%
IR	0.1396	0.1232	0.1291	0.1348	0.1396	0.1500	0.1425	0.1372	13%
LR	0.1478	0.1262	0.1318	0.1418	0.1459	0.1567	0.1501	0.1431	16%
IRKM	0.1307	0.1155	0.1182	0.1267	0.1318	0.1408	0.1346	0.1285	6.7%
LRKM	0.1419	0.1208	0.1275	0.1371	0.1386	0.1498	0.1443	0.1373	13%
DSP	0.1661	0.1662	0.1759	0.1605	0.1646	0.1724	0.1763	0.1689	29%

Note. The column “Avg.” measures the average MSE across all seven days of the test set, and the column “% Imp.” measures the percentage improvement (decrease) in average MSE from the IRT relative to each benchmark.

underlying segments’ bid landscapes. Notably, each benchmark using isotonic regression achieves better empirical performance than its logistic regression counterpart. This finding illustrates that isotonic regression models can offer substantial improvements in terms of predictive accuracy over other parametric approaches for bid landscape forecasting.

5. Conclusion

We propose a new framework for tractably training decision trees for the purposes of market segmentation and personalized decision-making which we call “Market Segmentation Trees” (MSTs).

While more traditional approaches to market segmentation (e.g., K -means) segment customers solely on the basis of their feature similarity, MSTs learn an *interpretable* market segmentation explicitly driven by identifying and grouping together customers with similar responses to personalized decisions. We propose a training algorithm for MSTs in which decision tree splits are recursively selected to optimize the predictive accuracy of the resulting collection of response models. We provide an open-source code base in Python which implements the training algorithm and can be easily customized to fit different personalized decision-making applications. We incorporate several strategies into the code base for improved scalability such as parallel processing and warm starts, and we provide a theoretical analysis of the code’s asymptotic computational complexity supporting its tractability in large data settings.

To demonstrate the versatility of our methodology, we design two new, specialized MST algorithms: (i) Choice Model Trees (CMTs) which can be used to predict a user’s choice amongst multiple options, and (ii) Isotonic Regression Trees (IRTs) which can be used to solve the bid landscape forecasting problem. We examine the performance of CMTs on a variety of synthetic datasets, observing that CMTs reliably find market segmentations which accurately predict choice probabilities, overcome model misspecification, and are robust to overfitting. We also apply our CMT algorithm to segment Expedia users and predict hotel bookings, and we find that the CMT consistently outperforms other natural benchmarks by 0.53-2.2% in hotel booking predictive accuracy. We then examine the performance of IRTs using a large-scale dataset from a leading Demand Side Platform (DSP), where we segment advertisement opportunities for users in order to predict auction win rate as a function of bid price. Our IRT algorithm consistently outperforms all benchmarks across 21 individual days of test data, notably achieving a 5-29% performance improvement over the DSP’s current approach.

Acknowledgments

Elmachtoub and McNellis were partially supported by NSF grant CMMI-1763000.

References

- Ali Aouad, Adam N Elmachtoub, Kris Ferreira, and Ryan McNellis. [n. d.]. GitHub repository. <https://github.com/rtm2130/MST>
- Lennart Baardman, Igor Levin, Georgia Perakis, and Divya Singhvi. 2017. Leveraging comparables for new product sales forecasting. *Available at SSRN 3086237* (2017).
- Fernando Bernstein, Sajad Modaresi, and Denis Sauré. 2018. A dynamic clustering approach to data-driven assortment personalization. *Management Science* (2018).
- Dimitris Bertsimas, Jack Dunn, and Nishanth Mundru. 2019. Optimal prescriptive trees. *INFORMS Journal on Optimization* (2019), ijoo-2018.

- Leo Breiman, Jerome Friedman, Charles J Stone, and Richard A Olshen. 1984. *Classification and regression trees*. CRC press, Chapter 10, 279–294.
- Andrew M Bruckner, E Ostrow, et al. 1962. Some function classes related to the class of convex functions. *Pacific J. Math.* 12, 4 (1962), 1203–1215.
- HD Brunk. 1970. Estimation of isotonic regression. *nonparametric Techniques in Statistical Inference. Cambridge Univ. Press* 177 (1970), 195.
- Kin-Yee Chan and Wei-Yin Loh. 2004. LOTUS: An algorithm for building accurate and comprehensible logistic regression trees. *Journal of Computational and Graphical Statistics* 13, 4 (2004), 826–852.
- Xi Chen, Zachary Owen, Clark Pixton, and David Simchi-Levi. 2015. A statistical learning approach to personalization in revenue management. *Available at SSRN 2579462* (2015).
- Gilbert A Churchill and Dawn Iacobucci. 2006. *Marketing research: methodological foundations*. Dryden Press New York.
- Dragos Florin Ciocan and Velibor V Mišić. 2018. Interpretable optimal stopping. *arXiv preprint arXiv:1812.07211* (2018).
- Adam N Elmachtoub, Ryan McNellis, Sechan Oh, and Marek Petrik. 2017. A Practical Method for Solving Contextual Bandit Problems Using Decision Trees. In *Proceedings of the Thirty-Third Conference on Uncertainty in Artificial Intelligence, UAI*. 11–15.
- Markus Ettl, Pavithra Harsha, Anna Papush, and Georgia Perakis. 2019. A data-driven approach to personalized bundle pricing and recommendation. *Manufacturing & Service Operations Management* (2019).
- Jerome Friedman, Trevor Hastie, and Robert Tibshirani. 2001. *The elements of statistical learning*. Vol. 1. Springer series in statistics Springer, Berlin.
- Bryce Goodman and Seth Flaxman. 2017. European Union regulations on algorithmic decision-making and a “right to explanation”. *AI Magazine* 38, 3 (2017), 50–57.
- Sachin Gupta and Pradeep K Chintagunta. 1994. On using demographic variables to determine segment membership in logit mixture models. *Journal of Marketing Research* 31, 1 (1994), 128–136.
- David Lee Hanson, Gordon Pledger, FT Wright, et al. 1973. On consistency in monotonic regression. *The Annals of Statistics* 1, 3 (1973), 401–421.
- ICDM. 2013. Personalized Expedia Hotel Searches. <https://www.kaggle.com/c/expedia-personalized-sort>
- Srikanth Jagabathula, Lakshminarayanan Subramanian, and Ashwin Venkataraman. 2018a. A Conditional Gradient Approach for Nonparametric Estimation of Mixing Distributions. (2018).
- Srikanth Jagabathula, Lakshminarayanan Subramanian, and Ashwin Venkataraman. 2018b. A Model-Based Embedding Technique for Segmenting Customers. *Operations Research* 66, 5 (2018), 1247–1267.

- Nathan Kallus. 2017. Recursive partitioning for personalization using observational data. In *Proceedings of the 34th International Conference on Machine Learning-Volume 70*. JMLR. org, 1789–1798.
- Wagner A Kamakura and Gary J Russell. 1989. A probabilistic choice model for market segmentation and elasticity structure. *Journal of marketing research* 26, 4 (1989), 379–390.
- Wagner A Kamakura, Michel Wedel, and Jagadish Agrawal. 1994. Concomitant variable latent class models for conjoint analysis. *International Journal of Research in Marketing* 11, 5 (1994), 451–464.
- Niels Landwehr, Mark Hall, and Eibe Frank. 2005. Logistic model trees. *Machine learning* 59, 1-2 (2005), 161–205.
- Hyafil Laurent and Ronald L Rivest. 1976. Constructing optimal binary decision trees is NP-complete. *Information processing letters* 5, 1 (1976), 15–17.
- Naresh Malhotra, John Hall, Mike Shaw, and Peter Oppenheim. 2006. *Marketing research: An applied orientation*. Pearson Education Australia.
- H Brendan McMahan, Gary Holt, David Sculley, Michael Young, Dietmar Ebner, Julian Grady, Lan Nie, Todd Phillips, Eugene Davydov, Daniel Golovin, et al. 2013. Ad click prediction: a view from the trenches. In *Proceedings of the 19th ACM SIGKDD international conference on Knowledge discovery and data mining*. ACM, 1222–1230.
- Velibor V Mišić. 2016. *Data, models and decisions for large-scale stochastic optimization problems*. Ph.D. Dissertation. Massachusetts Institute of Technology.
- John R Quinlan et al. 1992. Learning with continuous classes. In *5th Australian joint conference on artificial intelligence*, Vol. 92. World Scientific, 343–348.
- Sarah Sluis. 2019. Google Switches To First-Price Auction. AdExchanger. <https://adexchanger.com/online-advertising/google-switches-to-first-price-auction/>
- Kenneth E Train. 2009. *Discrete choice methods with simulation*. Cambridge university press, Chapter 2, 23–25.
- Michael N Tuma, Reinhold Decker, and Sören W Scholz. 2011. A survey of the challenges and pitfalls of cluster analysis application in market segmentation. *International Journal of Market Research* 53, 3 (2011), 391–414.
- Raluca M Ursu. 2018. The power of rankings: Quantifying the effect of rankings on online consumer search and purchase decisions. *Marketing Science* 37, 4 (2018), 530–552.
- Yuchen Wang, Kan Ren, Weinan Zhang, Jun Wang, and Yong Yu. 2016. Functional bid landscape forecasting for display advertising. In *Joint European Conference on Machine Learning and Knowledge Discovery in Databases*. Springer, 115–131.
- Jingyuan Yang, Chuanren Liu, Mingfei Teng, March Liao, and Hui Xiong. 2016. Buyer targeting optimization: A unified customer segmentation perspective. In *2016 IEEE International Conference on Big Data (Big Data)*. IEEE, 1262–1271.

Achim Zeileis, Torsten Hothorn, and Kurt Hornik. 2008. Model-based recursive partitioning. *Journal of Computational and Graphical Statistics* 17, 2 (2008), 492–514.

Appendix: Market Segmentation Trees

Appendix A: Proof of Theorem 1

We begin by providing an equivalent restatement of Theorem 1 which we refer to as Theorem A.1.

THEOREM A.1. *Assume $f(n, r)$ satisfies the following functional properties:*

ASSUMPTION A.1. *There exists an $M \geq 0$ and $C > 0$ such that $f(n, r) \leq C \cdot g(n, r)$ for all $n \geq M$.*

ASSUMPTION A.2. *$g(n, r)$ is continuous, monotonic nondecreasing, and convex in n for all $n \geq 0$.*

Then, assume that n is sufficiently large, meaning that Assumptions A.3 and A.4 are satisfied:

ASSUMPTION A.3. *$N_{\mathcal{T}}(D, l; n) \geq M$ for all l and \mathcal{T} .*

ASSUMPTION A.4. *For a fixed $\epsilon > 0$,*

$$g(n, r) \geq \frac{2(2^D - 1) - D}{D\epsilon} g(0, r) .$$

Then, the runtime of the MST's training algorithm is bounded by $(1 + \epsilon)DmCg(n, r)$.

Proof. We briefly outline the parallels between Theorem 1 and Theorem A.1 above. First, we argue that the assumptions of Theorem 1 imply the assumptions of Theorem A.1. Assumptions A.1 and A.2 are equivalent to Assumptions 1 and 2, respectively. Moreover, Assumptions 3 and 4 guarantee the existence of an n which satisfies Assumptions A.3 and A.4 for any fixed $\epsilon > 0$. We note that many runtime functions satisfy $g(0, r) = 0$ and thus Assumption A.4 is trivially satisfied for any $n > 0$ (as the monotonicity of $g(n, r)$ in n implies that $g(n, r) \geq 0$ for $n \geq 0$). For example, the runtime for linear regression, $O(nr^2 + r^3)$, can also be expressed as $O(nr^2)$ assuming that $n \geq r$, in which case $g(n, r) = nr^2$ and $g(0, r) = 0$. Of course, we could also apply Assumption A.4 to $g(n, r) = nr^2 + r^3$ and $g(0, r) = r^3$, in which case Assumption A.4 would relate the requisite magnitude of n for the theorem to hold to parameters r and D .

The conclusion of Theorem A.1 implies the conclusion of Theorem 1 – namely, that the runtime of the training algorithm is $O(D \cdot m \cdot g(n, r))$. Moreover, Theorem A.1 provides some additional insight into the magnitude of the constant behind the big O notation of Theorem 1. The conclusion of Theorem A.1 implies that the computational complexity of the MST's training algorithm is equivalent to that of fitting $(1 + \epsilon)Dm$ response models to the training data, and for sufficiently large n we may take ϵ to be arbitrarily small.

Our proof of Theorem A.1 (and Theorem 2 in the next section) relies on the following result from Bruckner et al. (1962):

LEMMA A.1. *Let $f(n)$ be a nonnegative, continuous, and convex function which satisfies $f(0) = 0$. Then,*

1. *$f(n)$ is star-shaped, i.e. $f(\alpha n) \leq \alpha f(n)$ for all $\alpha \in [0, 1]$ and for all $n \geq 0$.*
2. *$f(n)$ is superadditive, i.e. $f(n_1 + n_2) \geq f(n_1) + f(n_2)$ for all $n_1 \geq 0$ and $n_2 \geq 0$.*

We define the function $\tilde{g}(n, r) = g(n, r) - g(0, r)$, noting that Assumption A.2 implies that $g(0, r)$ is well-defined and finite. The properties of $\tilde{g}(n, r)$ are listed below:

1. $\tilde{g}(n, r)$ is continuous, monotonic nondecreasing, and convex in n for all $n \geq 0$ by Assumption A.2.
2. $\tilde{g}(0, r) = g(0, r) - g(0, r) = 0$.
3. $\tilde{g}(n, r) \geq \tilde{g}(0, r) = 0$ by monotonicity of $\tilde{g}(\cdot, r)$.
4. $\tilde{g}(n, r)$ is star-shaped and superadditive by the previous properties and Lemma A.1.

To prove the theorem, we first analyze the computational complexity of the split selection procedure of Eq. (4). Let $S(n, m, r)$ denote the runtime of the split selection procedure with respect to n observations, m binary contextual variables, and r response model parameters. The lemma below bounds the runtime of the split selection procedure when applied in each internal node of the trained MST \mathcal{T} .

LEMMA A.2. *If Assumptions A.1, A.2, and A.3 are satisfied, then for all $d \leq D-1$ and $l \in \{1, \dots, 2^d\}$,*

$$S(N_{\mathcal{T}}(d, l; n), m, r) \leq mC[\tilde{g}(N_{\mathcal{T}}(d, l; n), r) + 2g(0, r)]$$

Proof. To evaluate the quality of a candidate split, the split selection procedure fits response models within each of the resulting partitions from the split and computes the cumulative training error across the partitions. We first analyze the complexity of this “split evaluation” operation. Let n_1 and n_2 denote the number of observations in each of the split’s partitions, and note that $n_1 + n_2 = N_{\mathcal{T}}(d, l; n)$. Further, note that Assumption A.3 guarantees that $n_1 \geq M$ and $n_2 \geq M$, and more generally, that $N_{\mathcal{T}}(d, l; n) \geq M$ for all depths $d \leq D$, leaves l , and MSTs \mathcal{T} . Then, split evaluation takes time:

$$\begin{aligned} f(n_1, r) + f(n_2, r) &\leq C[g(n_1, r) + g(n_2, r)] \\ &= C[\tilde{g}(n_1, r) + \tilde{g}(n_2, r) + 2g(0, r)] \\ &\leq C[\tilde{g}(N_{\mathcal{T}}(d, l; n), r) + 2g(0, r)] \end{aligned}$$

Above, the first inequality uses Assumption A.1 and the fact that $n_1 \geq M$ and $n_2 \geq M$, the first equality applies the definition of \tilde{g} , and the second inequality uses the superadditivity of \tilde{g} . Since there are m binary contextual variables, there are m candidate splits which the split selection procedure must evaluate. Thus, the runtime for the split selection procedure is bounded by $mC[\tilde{g}(N_{\mathcal{T}}(d, l; n), r) + 2g(0, r)]$. \square

The split selection procedure is recursively applied through all internal nodes of the trained MST \mathcal{T} . Thus, the runtime of the training algorithm can be bounded as follows:

$$\begin{aligned} \sum_{d=0}^{D-1} \sum_{l=1}^{2^d} S(N_{\mathcal{T}}(d, l; n), r) &\leq mC \sum_{d=0}^{D-1} \sum_{l=1}^{2^d} \tilde{g}(N_{\mathcal{T}}(d, l; n), r) + 2 \sum_{l=1}^{2^d} g(0, r) \\ &\leq mC \sum_{d=0}^{D-1} \{\tilde{g}(n, r) + 2^{d+1}g(0, r)\} \\ &= mC[D\tilde{g}(n, r) + 2(2^D - 1)g(0, r)] \\ &= mC[Dg(n, r) + (2(2^D - 1) - D)g(0, r)] \\ &\leq mC[Dg(n, r) + D\epsilon g(n, r)] \\ &= mCD(1 + \epsilon)g(n, r) \end{aligned}$$

Above, the first inequality applies Lemma A.2 and the second inequality applies the superadditivity of \tilde{g} (noting that $\sum_{l=1}^{2^d} N_{\mathcal{T}}(d, l; n) = n$). The first equality is by algebra, the second equality applies the definition of \tilde{g} , the third inequality is by Assumption A.4, and the third equality is by algebra. This proves Theorem A.1, thereby proving Theorem 1. \square

Appendix B: Proof of Theorem 2

As in the previous section, we begin by providing an equivalent restatement of Theorem 2 which we refer to as Theorem B.1.

THEOREM B.1. *Assume $f(n, r)$ satisfies the following functional properties:*

ASSUMPTION B.1. *There exists an $M_1 \geq 0$ and $C_1 > 0$ such that $f(n, r) \leq C_1 g(n, r)$ for all $n \geq M_1$.*

ASSUMPTION B.2. *$g(n, r)$ is continuous, monotonic nondecreasing, and convex in n for all $n \geq 0$.*

ASSUMPTION B.3. *Let \mathcal{T} denote the trained MST. There exists an $M_2 \geq 0$ and $C_2 > 0$ such that for all $d \in \{0, \dots, D-1\}$ and $l \in \{1, \dots, 2^d\}$, $N_{\mathcal{T}}(d, l; n) \leq C_2 n / 2^d$ for all $n \geq M_2$.*

ASSUMPTION B.4. *There exists an $M_3 \geq 0$ and $C_3 > 0$ such that $g(C_2 n, r) \leq C_3 g(n, r)$ for all $n \geq M_3$.*

Then, assume that n is sufficiently large, defined by satisfying the following properties:

ASSUMPTION B.5. *$N_{\mathcal{T}}(D, l; n) \geq M_1$ for all l and T .*

ASSUMPTION B.6. *$n \geq \max\{M_2, 2^{D-1} M_3\}$.*

ASSUMPTION B.7. *For a fixed $\epsilon > 0$,*

$$g(n, r) \geq \frac{h(C_3, D, Q)}{\epsilon} g(0, r) ,$$

where $h(C_3, D, Q)$ is a function of C_3 , D , and Q .

Then, the runtime of the MST's training algorithm with parallel processing is bounded by

$$(1 + \epsilon) C_3 (D/Q + 2) m C_1 g(n, r) .$$

Proof. We first discuss how the assumptions of Theorem 2 imply those of Theorem B.1. Assumptions B.1, B.2, B.3, and B.4 are a rephrasing of Assumptions 1, 2, 5, and 6, respectively. Moreover, Assumptions 3 and 4 guarantee the existence of a sufficiently large n which satisfies Assumptions B.5, B.6, and B.7 for any fixed $\epsilon > 0$. As in the previous section, we again note that many runtime functions satisfy $g(0, r) = 0$ and thus Assumption B.7 would be trivially satisfied for all $n \geq 0$.

The conclusion of Theorem B.1 implies that the runtime of the training procedure with parallel processing can be bounded by

$$\begin{aligned} & (1 + \epsilon) C_1 C_3 (D/Q + 2) m g(n, r) \\ & \leq (1 + \epsilon) C_1 C_3 (\max\{D/Q, 1\} + 2 \max\{D/Q, 1\}) m g(n, r) \\ & = 3(1 + \epsilon) C_1 C_3 \max\{D/Q, 1\} m g(n, r) . \end{aligned}$$

Thus, Theorem B.1 implies that the computational complexity of the training procedure can be expressed as $O(\max\{D/Q, 1\} m g(n, r))$, which is precisely the conclusion of Theorem 2.

As in the proof of Theorem A.1, we begin by bounding the runtime of the split selection procedure of Eq. (4). Let $\tilde{g}(n, r) = g(n, r) - g(0, r)$, and let $S(n, m, r)$ denote the runtime of the split selection procedure on n observations, m binary contextual variables, and r response model parameters. Lemma B.1 below bounds the split selection procedure's runtime for each internal node of the trained MST \mathcal{T} .

LEMMA B.1. *If Assumptions B.1, B.2, B.3, B.4, B.5, and B.6 are satisfied, then for all $d \leq D-1$ and $l \in \{1, \dots, 2^d\}$,*

$$S(N_{\mathcal{T}}(d, l; n), m, r) \leq m C_1 [(C_3 / 2^d) \tilde{g}(n, r) + (C_3 + 1) g(0, r)] .$$

Proof. Noting that Assumptions B.1, B.2, and B.5 are equivalent to Assumptions A.1, A.2, and A.3, respectively, we apply Lemma A.2 to arrive at the first inequality in the chain of inequalities below:

$$\begin{aligned}
S(N_{\mathcal{T}}(d, l; n), m, r) &\leq mC_1 [\tilde{g}(N_{\mathcal{T}}(d, l; n), r) + 2g(0, r)] \\
&= mC_1 [g(N_{\mathcal{T}}(d, l; n), r) + g(0, r)] \\
&\leq mC_1 [g(C_2 n / 2^d, r) + g(0, r)] \\
&\leq mC_1 [C_3 g(n / 2^d, r) + g(0, r)] \\
&= mC_1 [C_3 \tilde{g}(n / 2^d, r) + (C_3 + 1)g(0, r)] \\
&\leq mC_1 [(C_3 / 2^d) \tilde{g}(n, r) + (C_3 + 1)g(0, r)]
\end{aligned}$$

Above, the first equality applies the definition of \tilde{g} , the second inequality applies Assumptions B.3 and B.6 and the monotonicity of g in n , the third inequality applies Assumptions B.4 and B.6, the second equality applies the definition of \tilde{g} , and the fourth inequality applies the star-shaped property of \tilde{g} (discussed in the previous section). \square

The split selection procedure is applied to each internal node (d, l) of the MST for $d \in \{0, \dots, D-1\}$ and for $l \in \{1, \dots, 2^d\}$. We next bound the runtime of applying the split selection procedure to all nodes l at a given depth d . Recall that our training algorithm parallelizes these 2^d procedures across the available computational cores Q . The total runtime of this parallelization scheme is upper bounded by the following job scheduling process. Assume that the 2^d split selection procedures (“jobs”) are run in batches of Q (one job per core), and the next batch of Q jobs are run only when all jobs in the current batch have terminated. There would then be $\lceil \frac{2^d}{Q} \rceil$ total batches, and the runtime of each individual job (and thus each batch) can be bound by Lemma B.1. Thus, the runtime of parallelizing all 2^d split selection procedures at depth d can be bound by:

$$\left\lceil \frac{2^d}{Q} \right\rceil mC_1 \left[\frac{C_3}{2^d} \tilde{g}(n, r) + (C_3 + 1)g(0, r) \right] =: \left\lceil \frac{2^d}{Q} \right\rceil \left[\frac{K_1}{2^d} + K_2 \right]$$

where in what follows we define $K_1 = mC_1 C_3 \tilde{g}(n, r)$ and $K_2 = mC_1 (C_3 + 1)g(0, r)$ for notational convenience. Finally, the runtime of the MST’s training procedure is equal to the runtimes of the split selection procedures across all depths $d \in \{0, \dots, D-1\}$ of the MST, which can be bounded as follows:

$$\begin{aligned}
&\sum_{d=0}^{D-1} \left\lceil \frac{2^d}{Q} \right\rceil \left[\frac{K_1}{2^d} + K_2 \right] \\
&\leq \sum_{d=0}^{D-1} \left(\frac{2^d}{Q} + 1 \right) \left[\frac{K_1}{2^d} + K_2 \right] \\
&= \sum_{d=0}^{D-1} \left\{ \frac{K_1}{Q} + \frac{K_1}{2^d} + K_2 + \frac{2^d K_2}{Q} \right\} \\
&= \frac{DK_1}{Q} + 2 \left(1 - \frac{1}{2^D} \right) K_1 + DK_2 + \frac{(2^D - 1)K_2}{Q} \\
&\leq \frac{DK_1}{Q} + 2K_1 + DK_2 + \frac{(2^D - 1)K_2}{Q} \\
&= \left(\frac{D}{Q} + 2 \right) mC_1 C_3 \tilde{g}(n, r) + \left(D + \frac{2^D - 1}{Q} \right) mC_1 (C_3 + 1)g(0, r)
\end{aligned}$$

$$\begin{aligned}
&= mC_1 \left[\left(\frac{D}{Q} + 2 \right) C_3 g(n, r) + \left[\left(D + \frac{2^D - 1}{Q} \right) (C_3 + 1) - \left(\frac{D}{Q} + 2 \right) C_3 \right] g(0, r) \right] \\
&\leq mC_1 \left[\left(\frac{D}{Q} + 2 \right) C_3 g(n, r) + \epsilon \left(\frac{D}{Q} + 2 \right) C_3 g(n, r) \right] \\
&= (1 + \epsilon) mC_1 \left(\frac{D}{Q} + 2 \right) C_3 g(n, r)
\end{aligned}$$

Above, the first two inequalities and the first three equalities are by algebra, and the fourth equality is by applying the definition of \tilde{g} . The third inequality applies Assumption B.7 with

$$h(C_3, D, Q) = \frac{\left(D + \frac{2^D - 1}{Q} \right) (C_3 + 1) - \left(\frac{D}{Q} + 2 \right) C_3}{\left(\frac{D}{Q} + 2 \right) C_3}.$$

Finally, the last equality is by algebra. This proves Theorem B.1 and thus Theorem 2. \square

Appendix C: Details of Datasets Used in Section 4

C.1. Details of Dataset Generation for Section 4.1.1

Below we provide details on how each dataset is generated for each of the three ground truth models summarized in Section 4.1.1.

Context-Free MNL: We generate the MNL’s parameter vector β by sampling each element of β independently from a Uniform(-1,1) distribution. This MNL model is used to generate the choices for all users in the dataset. Each user is encoded by four contextual variables sampled independently from a Uniform(0,1) distribution. The number of options offered to each user is sampled uniformly-at-random from the set $\{2, 3, 4, 5\}$, and each option is encoded by four features which are sampled independently from a Uniform(0,1) distribution for each user. Choices are simulated from the probability distribution specified by the MNL model given the assortment – in particular, the contextual variables are *not* considered when generating choices.

Choice Model Tree: First, the number of leaf nodes is sampled uniformly-at-random from the set $\{4, 5, 6, 7\}$. Then, a CMT of depth at most three is randomly constructed which has the target number of leaf nodes. Recall that each (numeric) split of a CMT is encoded by a splitting variable and split point (e.g., “ $x_3 < 0.4$ ”). All splitting variables and split points contained in the CMT are sampled uniformly-at-random with the constraint that each split is roughly “balanced”, defined as the left and right children of the split containing at least 30% of the contexts mapped to their parent. Each leaf contains an MNL instance whose parameter vector β is generated by sampling each element of β independently from a Uniform(-1,1) distribution. Contexts and options are generated in the same manner as they were for the Context-Free MNL ground truth model, with contextual features and options being sampled independently from a Uniform(0,1) distribution. Choices are generated for each user by (1) mapping the user to the leaf of the CMT corresponding to the user’s context, and (2) sampling a choice from the user’s offered assortment using the leaf’s MNL model.

K-Means Clustering Model: First, the number of clusters K is sampled uniformly-at-random from the set of values $\{4, 5, 6, 7\}$; recall that we also used this set of values to sample the number of leaves present in the CMT ground truth model. Each cluster $k \in \{1, \dots, K\}$ has an associated MNL model whose parameter vector β_k is generated by sampling each element of β_k independently from a Uniform(-1,1) distribution. Furthermore, each cluster also has an associated “mean context vector” \bar{x}_k whose entries are sampled independently from a

Uniform(0,1) distribution. We next define a probability mass function (p.m.f.) $\pi = \{\pi_1, \dots, \pi_K\}$ over the K clusters, where π_k denotes the probability that a user belongs to cluster k . We generate the p.m.f. through the following procedure:

1. For each cluster $k \in \{1, \dots, K\}$, sample $U_k \in \mathbb{R}$ from a Uniform(-1,1) distribution.
2. Let $\pi_k := \frac{\exp(U_k)}{\sum_{k'=1}^K \exp(U_{k'})}$ for all $k \in \{1, \dots, K\}$.

Options are generated through the same procedure as in the other two ground truth models, with option features being sampled independently from a Uniform(0,1) distribution. Contexts and choices are generated for each user in the following manner:

1. Sample the cluster $k \in \{1, \dots, K\}$ belonging to the user from p.m.f. π .
2. Sample the user's context vector from a multivariate normal distribution with mean parameter \bar{x}_k and covariance $\sigma^2 I$, where I denotes the identity matrix. Here, $\sigma = 0.08$ is configured to ensure that there is an adequate separation between contexts belonging to different clusters.
3. Sample the user's choice from the MNL model associated with cluster k , i.e. the MNL model with parameter vector β_k .

C.2. Description of Expedia Hotel Booking Dataset for Section 4.1.2

The number of hotels in the displayed assortments varies between 1 and 38, with the most common assortment sizes being between 31 and 35. In addition, the no-purchase option is incorporated into our model as one potential choice outcome for each search instance. The original published version of the dataset only contains searches resulting in at least one hotel click, and 69% of reported searches result in a hotel booking. Since this is an unusually high conversion rate, it is suspected that such searches leading to a transaction have been oversampled (Ursu 2018). There are a few hotels with unusually high prices in the dataset (e.g., \$19 million per night) which are suspected to be due to price reporting errors (Ursu 2018). To correct for this, we remove any hotels from the assortments with prices of over \$4,000 per night.

The CMT uses seven contextual features pertaining to the user and search query for the purposes of market segmentation. The features representing x , detailed below, are reported alongside their original published feature names.

- *Information regarding the user:* Number of adults (`srch_adults_count`) and number of children (`srch_children_count`) in the user's party.
- *Information regarding the user's search query:* Duration of hotel stay (`srch_length_of_stay`), number of days between the search date and the hotel stay (`srch_booking_window`), number of hotel rooms specified in the search (`srch_room_count`), indicator for whether the stay includes a Saturday night (`srch_saturday_night_bool`), and ID (`site_id`) of the Expedia point of sale (e.g., Expedia.com, Expedia.co.uk, Expedia.co.jp). The features `srch_saturday_night_bool` and `site_id` are treated as categorical in the CMT, while all other features are treated as numeric.

The MNL response models of the CMT utilize the following hotel information in modeling booking utilities. As above, we report each hotel feature, corresponding to p , alongside its published name.

- *Hotel price information:* The display price of the hotel (`price_usd`), the logarithm of the mean price of the hotel over the last trading period (`prop_log_historical_price`), and an indicator for whether the hotel had a sale price promotion specifically displayed (`promotion_flag`).

- *Hotel quality and brand information:* The star rating of the hotel (`prop_starrating`), the mean customer review score for the hotel (`prop_review_score`), a score outlining the desirability of a hotel’s location (`prop_location_score1`), and whether the hotel is part of a major hotel chain (`prop_brand_bool`).

- *Hotel display information:* The hotel’s rank position on Expedia’s search results page (`position`). In addition to the raw position number, we also include three indicators for whether a hotel is in rank positions 1-5, 6-10, and 11-15.

C.3. Description of DSP Dataset for Section 4.2

There are ten user and ad spot auction features used as contexts for segmentation which can be categorized as follows:

- *Information regarding the ad spot:* Area and aspect ratio of the ad spot (defined as “width×height” and “width/height”, respectively), ad spot fold position (defined as whether the ad is visible without scrolling), and ID of the encompassing site. Area and aspect ratio are treated as numeric features in the IRT; all other reported features are treated as categorical. Due to the high dimensionality of the site IDs (with thousands of unique values per exchange), we first pre-cluster the site IDs before applying the IRT and the benchmark algorithms to the training data.

- *Information regarding the user’s site visit:* Time-of-day and day-of-week of the user’s site visit, country of the visiting user, and ad channel from which the user arrived (e.g., video, mobile, search).

- *Information regarding private marketplace deals:* ID encoding a private deal between an advertiser and a publisher which might affect the dynamics of the auction.